Cover Letter

Dear Mr. Editor,

We are hereby submitting the response for the referees comments for the manuscript under the title “Stratospheric ozone and QBO interaction with the tropical troposphere on intraseasonal and interanual time-scales: a wave interaction perspective”.

We have attempted to give a detailed answer to each of the points raised by the referees as well as the public short comment. Some of the referees’ comments lead to major improvements on this work. Here we summarize the main points:

- Following the suggestion of Referee #2 we have included a composite analysis showing the evolution of each of the normal mode components of the MJO (Kelvin and Rossby). The composite analysis was done separately for each of the QBO phases and shows that there are strong and statistically significant changes in the dynamical fields (velocity and geopotential height) associated with the waves depending on the QBO phase. This this new section replaces the old section on the topographic forced gravity waves.
- Referee #3 pointed out to a pre-processing problem on the fast timescale PDC analysis, this was corrected and an improved version of the figure were included.
- A detailed description of the asymptotic statistics of the PDC and the calculation of confidence intervals was included following the suggestions of referees #1 and #2.

We finally would like to thank all the referees and the editor for the comments that lead to a substantial improvement of our work.

Yours sincerely,

Breno Raphaldini

Referee 1

(1)I think the statistics of the method need to be much more carefully described. At the moment, we aren't really given any indication of how the significance is determined other than a reference to another article. One thing I am particularly concerned about is that by doing this frequency decomposition as well as using multiple variables, it means that effectively a very large number of tests has been performed. Is this accounted for when performing the significance tests. For example, if you test 100 different frequencies and use a 95% level, you'd expect 5 different frequencies to show a significant signal. Furthermore, how is autocorrelation in the time series for the low frequencies accounted for in the significance testing. For the decadal timescales there will be very few degrees of freedom in the observational record and I would hope that this is being accounted for in the statistical testing but it's not clear. So, I strongly recommend an improved discussion of the statistical testing and the significance of results in light of these complicating factors.

R: R: We apologize that we did not describe the statistics with sufficient details. PDC is a function of the coefficients of vector autoregressive model. Given that the coeffcients are asymptotically jointly normally distributed, we can use the delta method (Serfling, 1980) to analytically calculate the asymptotic statistics for PDC. After a straightforward but tedious algebraic computation, we can show that PDC at frequency lambda is distributed asymptotically (under the null hypothesis of zero PDC) as the weighted sum of two chi-square with one degree of freedom (Takahashi et al., 2007). Therefore, we can use this asymptotic distribution to calculate the p-values. For details of the derivation, we refer to Takahashi et al. (2007). Significance levels for frequency domain quantities are controlled only point-wise as this is the standard everywhere. The reason for this is that the point estimates for neighboring frequencies are highly correlated. Therefore, standard correction like bonferroni or even FDR that assume independence or weak dependence give the wrong significance level. Every single article that we found where PDC, coherence or bi-coherence were used and the significance level is reported use the frequency-wise significance level (for representative examples see Huybers and Curry, 2006 and Came et al., 2007). For PDC it is easy to see that the use of frequency-wise significance level is reasonable given that the PDC values for different frequencies are the Fourier transform of the same coefficients of the autoregressive process. The fact that lower frequency have fewer samples are taken care by higher threshold values for PDC at lower frequencies. We added the following brief description of the statistics for PDC in the main text. "PDC is a function of the coefficients of vector autoregressive model. Given that the coefficients are asymptotically jointly normally distributed, we can use the delta method (Serfling, 1980) to obtain analytically the asymptotic statistics for PDC. After an algebraic computation, we can show that PDC at frequency lambda is distributed asymptotically (under the null hypothesis of zero PDC) as the weighted sum of two chi-square with one degree of freedom (Takahashi et al., 2007). Therefore, we can use the asymptotic distribution to calculate the p-value. For details of the derivation, we refer to Takahashi et al. (2007). The significance level used in the article for PDC is the frequency-wise value as it is the standard for frequency domain analysis given the high correlation between the point estimates for neighboring frequencies (see e.g. Huybers and Curry, 2006; Came et al., 2007)."

(2) I question whether showing the interaction between the gravity waves and the MJO is really an explanation. At pg 2, l3, it is stated that this connection represents a partial explanation, but it's not really a mechanistic understanding. It certainly hints at something that should be investigated, but I wouldn't even call it a partial explanation. One aspect I'm concerned about with this inference is whether the stratospheric zonal winds are accounted for when assessing the connection between the gravity waves and the MJO or not. It's not entirely clear to me. Is the connection between the gravity waves and the MJO just a simple assessment of the connection between the gravity waves and the MJO or is it an assessment of whether the gravity waves provide you more information beyond what you'd already get given the connection between the stratospheric zonal wind and the MJO. If it is not the latter, then isn't it possible that this connection between the gravity waves and the MJO simply represent the connection between the QBO and the MJO where the gravity wave variability is a signal of the QBO and not necessarily connected to the MJO in a causal sense.

R:The idea to investigate the effect of QBO related normal modes with MJO related normal modes was inspired by the works on nonlinear resonance as a driver for MJO through the interaction of tropics-extra tropics,see : Raupp, C. F., & Dias, P. L. S. (2010). Interaction of equatorial waves through resonance with the diurnal cycle of tropical heating. Tellus A: Dynamic Meteorology and Oceanography, 62(5), 706-718/ -Majda, A. J., & Biello, J. A. (2003). The nonlinear interaction of barotropic and equatorial baroclinic Rossby waves. Journal of the atmospheric sciences, 60(15), 1809-1821.). The idea then is to search for evidence for mode interaction that may lead to stratosphere-troposphere interaction similar to the aforementioned theories for the interaction tropics-extratropics. In this sense our work may be regarded and a evidence for such a mechanism, although we do not develop the theory itself. Regarding the information of the interaction of gravity waves on MJO. The normal modes that contribute to the QBO are determined by a linear regression procedure, gravity waves being some of the main contributors. To say that gravity waves associated with the QBO also interact with the QBO gives more information on the MJO-QBO interaction since it restricts the type of mode responsible for the interaction, in this particular case gravity modes rather than balanced (Rossby) modes.

3) Conclusions are drawn about what factors influence the MJO on what frequencies. I wonder if, having performed this causality analysis, which I expect will seem like a bit of a black box to many readers, whether the results could then be related back to something a bit more physical e.g., could you present the time series and lagged correlations between the fields at the relevant frequencies to convince readers of the actual correlation between these time series.

R:In the present version of the manuscript we have included a composite analysis based on Reviwer #2 suggestion showing the differences on each normal mode component of the the MJO depending on the phase of the QBO.

4) I’m not entirely sure what is shown in Fig 12, but it looks kind of strange. It is described by "We recompose the zonal wind fields of WIG waves associated with the QBO". Is this showing where the amplitude of the gravity waves fluctuate along with the QBO? So it’s really showing where orographically generated gravity waves are active? If so, it makes sense that there should be such a close correspondence between orography and this metric. But is it really the case that gravity waves over Greenland and Antarctica are varying with the QBO? Furthermore, I don’t think it’s really the orographic gravity waves that interact with the QBO, it’s more the convectively generated gravity waves, which we don’t really see in this figure. I think this all needs a bit more explanation and a bit more discussion of the physical linkages to complement the Partial Directed Coherence analysis.

R: After discussion with the co-authors we decided to remove this section on the spatial structure of the gravity waves, since we came to the conclusion that it was not bringing insight into the main problem of the article. Instead we followed the Reviewer #2 suggestion to present composites of the MJO related normal modes for each MJO phase, comparing them as a function of the phase of the QBO (positive or negative).

1)I am concerned about the use of the Granger causality method since this assumes linear dynamics and Gaussian statistics. The MJO is probably a non-linear phenomenon. Did you also test the convergent cross-mapping approach by Sugihara? In a recently published studies we have shown that time-lagged CCM and machine learning approaches are much better: Huang, Y., C. Franzke, N. Yuan and Z. Fu, C1 ESDD Interactive comment Printer-friendly version Discussion paper 2020: Systematic identification of causal relations in high-dimensional chaotic systems: Application to Stratopshere-Troposphere coupling. Clim. Dyn., in press. https://link.springer.com/article/10.1007/s00382-020-05394-0Huang, Y., Z. Fu and C. Franzke, 2020: Detecting causality from time series in a machine learning framework. Chaos, 30, 063116.

R: In this article, we have used the PDC method to infer Granger causality between multiple time-series in the frequency domain. The main advantage of PDC and Granger causality is that it is theoretically related to the mutual information rate (MIR) between signals (see Takahashi et. al 2010 Information theoretic interpretation of frequency domain connectivity measures.

Biological Cybernetics, v.103, p. 463-469, 2010.; Geweke, J. F. (1984). Measures of conditional linear dependence and feedback between time series. *Journal of the American Statistical Association*, *79*(388), 907-915.). Information-theoretic quantities are usually costly to estimate directly from time-series since it relies on the estimation of multi-dimensional probability distributions. As proved in Takahashi et. al 2010, PDC is a Gaussian approximation to the MIR. This means that if the time-series are stationary and Gaussian PDC provides an exact estimate for the MIR, when the time-series are not Gaussian (possibly due to underlying nonlinearities) the PDC will capture part but not all of the information flow between the time-series.
There are many "causality" estimation methods in the literature, all of them with some advantages and drawbacks. Among the several causality detection methods the Convergent-Cross Mapping (CCM) method is proposed as a method that is capable to capture couplings in highly-nonlinear settings since it relies phase-space embedding procedures. CCM. However, it comes with a few drawbacks that would require more in-depth investigation before we could apply it in the present setting, namely:

(1) CCM is a bi-variate measure. Granger causality and PDC are genuinely multivariate measures.
(2) CCM may lead to wrong or misleading results when moderate to high levels of noise are present (see Mønster, D., Fusaroli, R., Tylén, K., Roepstorff, A., & Sherson, J. F. (2017). Causal inference from noisy time-series data—Testing the Convergent Cross-Mapping algorithm in the presence of noise and external influence. *Future Generation Computer Systems*, *73*, 52-62.). Granger causality and PDC are designed to work for signals with stochasticity.
(3) CCM does not have an automated way to decide the optimal lag between time series. Granger causality and PDC are based on autoregessive process in which order estimation is well studied.
(4) There are no theoretical guarantees for the statistical properties of CCM. Both PDC and Granger causality are at very well studied measures in which there are thousands of articles applying it and we understand well their statistical properties (Lutkepohl, 2005; Takahashi et al., 2007).

> Finally, although PDC is a stochastic linear method, it correctly reconstruct the topology of networks of nonlinear oscillators (see Winterhalder, M., Schelter, B., & Timmer, J. (2007). Detecting coupling directions in multivariate oscillatory systems. *International Journal of Bifurcation and Chaos*, *17*(10), 3735-3739.), Moreover, it has been successfully and extensively used to infer information flow in highly nonlinear time-series data in neuroscience (Bressler, S. L., & Seth, A. K. (2011). Wiener–Granger causality: a well established methodology. *Neuroimage*, *58*(2), 323-329.). The fact that PDC can detect nonlinear interactions is not difficult to understand, given that linear regression also can see nonlinear interaction unless the nonlinearity is highly non-monotonic.

2) It is not really clear to me how you compute the time series you then use for the analysis. Are these just the projections of particular normal modes? If yes, how many normal modes do you use to represent the MJO and QBO? Or do you use just one normal mode for the respective wave type?

R:The time-series associated with the normal modes that we used correspond the the energy of a group of modes defined by:

$$E(t) = \frac{1}{2}\sum_{m=1}^{M} gD_m \sum_{k=0}^{K}\sum_{n=0}^{N}([\chi_{kmn}(t)]^{*}\chi_{kmn}(t))$$

Where g is the acceleration of gravity, D_m is the equivalent height of the m-th vertical index, $\chi_{kmn}(t)$ is the complex amplitude of the normal mode with zonal wave number k, meridional index n and vertical index m. M=43, K=32 and N are the respective truncation numbers for each index. For the MJO we selected the three first three even meridional indices for the Rossby modes (no selection on the vertical and zonal modes).

3) While the MJO normal modes have large amplitudes during MJO events and the set of normal modes are also then coherent. However, the normal modes can also have large amplitudes during non-MJO/QBO events. So, I think your results on the MJO time scale might be robust but I am not sure whether your results are related to the MJO on longer time scales; there probably is an effect of the QBO/ozone on the particular normal modes but I do not think you have shown that this is really related to the MJO.

In the present version of the manuscript we have included the composite analysis as suggested by this referee. This analysis clearly shows a difference in the long term behavior of the MJO-related modes, this was done for the QBO timescale (~28 months), and probably accounts for the causality between QBO modes and MJO modes at this time scale. Differences at other time-scales such as the solar cycle timescale still need to the investigated in more detail.

4) The quality of some of the figures is rather poor (Figs. 3, 10, 11).

R:Due to the large number of figures we were having problems compiling the file, which lead us to include figures with lower resolution, in the new version of the manuscript we included figures with better resolution.

5) What do the diagonal plots in Fig. 1 represent? Is that the causality of the time series with itself? What can I learn from this?

R:The diagonal plots correspond to the power spectrum of each of the variables, which is equivalent to the PDC of between the variable and itself.

6) How do you compute the significance of the causal relations? A brief description would be useful.

R:In this version of the manuscript we have included a description of the statistics, in particular how we obtain the conficence intervals of the PDC. We refer back to our response to the first question of referee #1.

“We apologize that we did not describe the statistics with sufficient details. PDC is a function of the coefficients of vector autoregressive model. Given that the coeffcients are asymptotically jointly normally distributed, we can use the delta method (Serfling, 1980) to analytically calculate the asymptotic statistics for PDC. After a straighforward but tedious algebraic computation, we can show that PDC at frequency lambda is distributed asymptotically (under the null hypothesis of zero PDC) as the weighted sum of two chi-square with one degree of freedom (Takahashi et al., 2007). Therefore, we can use this asymptotic distribution to calculate the p-values. For details of the derivation, we refer to Takahashi et al. (2007).

Significance levels for frequency domain quantities are controled only point-wise as this is the standard everywhere. The reason for this is that the point estimates for neighboring frequencies are highly correlated. Therefore, standard correction like bonferroni or even FDR that assume independence or weak dependence give the wrong signficance level. Every single article that we found where PDC, coherence or bi-coherence were used and the signficance level is reported use the frequency-wise significance level (for representative examples see Huybers and Curry, 2006 and Came et al., 2007). For PDC it is easy to see that the use of frequency-wise significance level is reasonable given that the PDC values for different frequencies are the fourier transform of the same coefficents of the autoregressive process. The fact that lower frequency have fewer samples are taken care by higher threshold values for PDC at lower frequencies. We added the following brief description of the statistics for PDC in the main text.

“PDC is a function of the coefficients of vector autoregressive model. Given that the coeffcients are asymptotically jointly normally distributed, we can use the delta method (Serfling, 1980) to obtain analytically the asymptotic statistics for PDC. After na algebraic computation we can show that PDC at frequency lambda is distributed asymptotically (under the null hypothesis of zero PDC) as the weighted sum of two chi-square with one degree of freedom (Takahashi et al., 2007). Therefore, we can use the the asymptotic distribution to calculate the p-value. For details of the derivation, we refer to Takahashi et al. (2007). The significance level used in the article for PDC is the frequency-wise value as it is the standard for frequency domain analysis given the high correlation between the point estimates for neighboring frequencies (see e.g. Huybers and Curry, 2006; Came et al., 2007)."

"

7) There is a recent paper: Franzke, C., D. Jelic, S. Lee and S. Feldstein, 2019: Systematic Decomposition of the MJO and its Northern Hemispheric Extra-Tropical Response into Rossby and Inertio-Gravity Components. Q. J. Roy. Meteorol. Soc., 145, 1147-1164. They use a composite approach which might be better suited to investigate the MJO and QBO. Using linear regression might mix too many non-events into the analysis. C2 ESDD Interactive comment Printer-friendly version Discussion paper.

R:In the present version of the manuscript we have included an analysis derived from the reference suggest by the referee "Systematic Decomposition of the MJO and its Northern Hemispheric Extra-Tropical Response into Rossby and Inertio-Gravity Components. Q. J. Roy. Meteorol. Soc., 145, 1147-1164.". We believe that this analysis has lead to a better understanding of how the QBO affects each normal mode component of the MJO (ROT and Kelvin). In what follows we include the corresponding figures with corresponding descriptions.

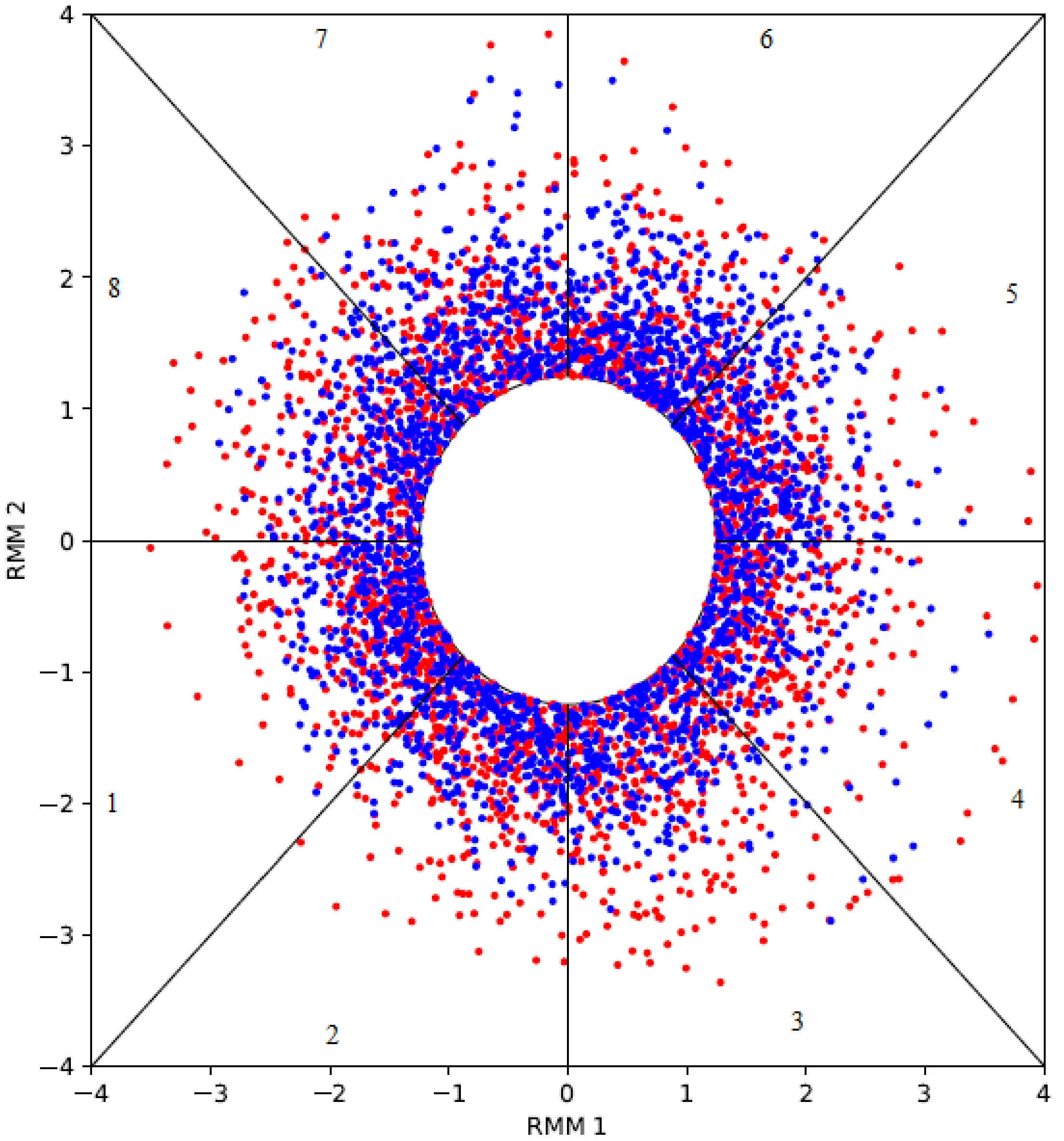

Figure 2.7.1: MJO phase diagram showing all points (days) in which $(RMM_1^2 + RMM_1^2 \geq 1)$. Points marked in red

In order to exclude the cases in which the RMM index is not associated with a MJO event we excluded all cases in which $(RMM_1^2 + RMM_1^2 < 1)$., among those cases we separated the ones for which the stratospheric zonal wind at 30Mb was positive (red) and negative (blue) in the figure 2.7.1. The MJO phase diagram was divided into 8 phases as in Franzke et. al 2019. For which QBO (positive or negative) state and for which MJO phase (i=1,2,…,8) we calculated the mean velocity and pressure fields associated with ROT and Kelvin modes at 200 Mb.

Figures 2.7.2 and 2.7.3 are display respectively the composites associated with the reconstructions of velocity and geopotential height fields associated with ROT modes for each of the 8 MJO phases with positive stratospheric zonal wind at 30 mb (SZW30+) and negative (SZW30+). In order to compare both composites we compute the difference between SZW30+ and SZW30- of each field for each MJO phase. This is displayed in figure 2.7.4. We notice that for phases 1-3 the difference (of the geopotential height fields represented by the hatched region) is statistically significant for almost the entire domain. For phase 4 the fields are more similar with small regions with significant difference, associated with Rossby double vortices. Between phases 5-8 the areas with significant difference become larger again.

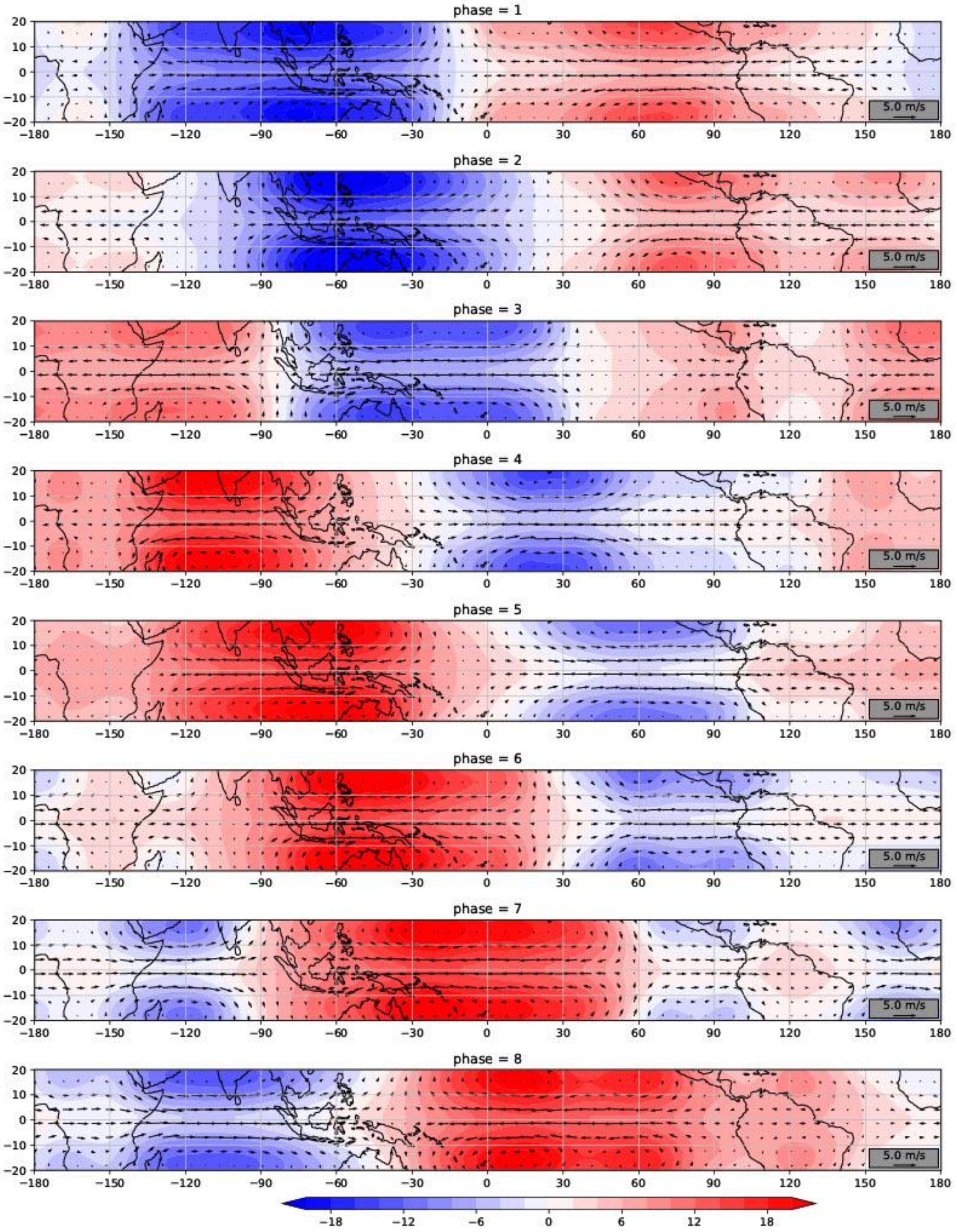

Figure 2.7.2: Reconstruction of the velocity and geopotential height fields associated with ROT modes with SZW30+ at 200 Mb.

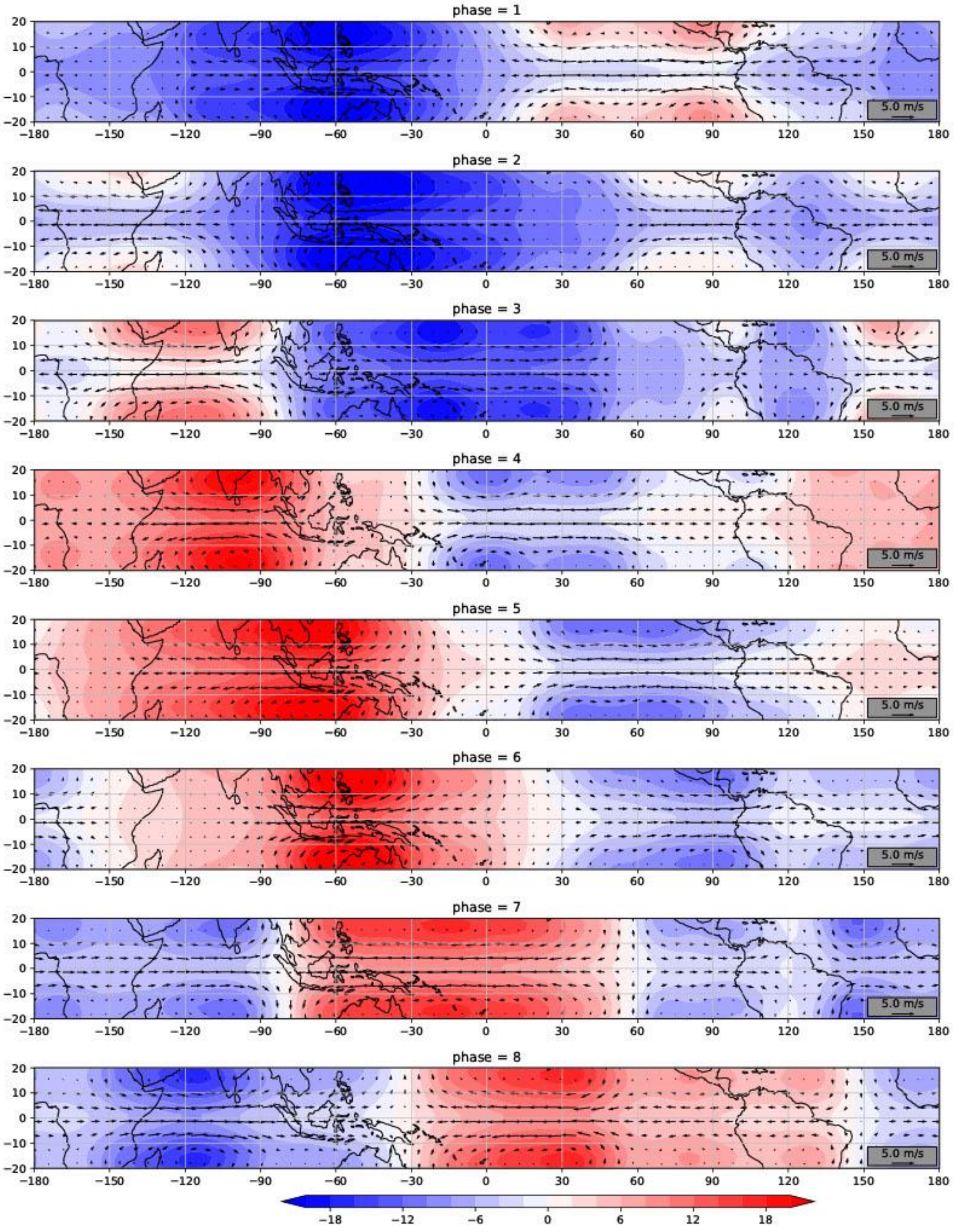

Figure 2.7.3: Reconstruction of the velocity and geopotential height fields associated with ROT modes with SZW30- at 200 Mb.

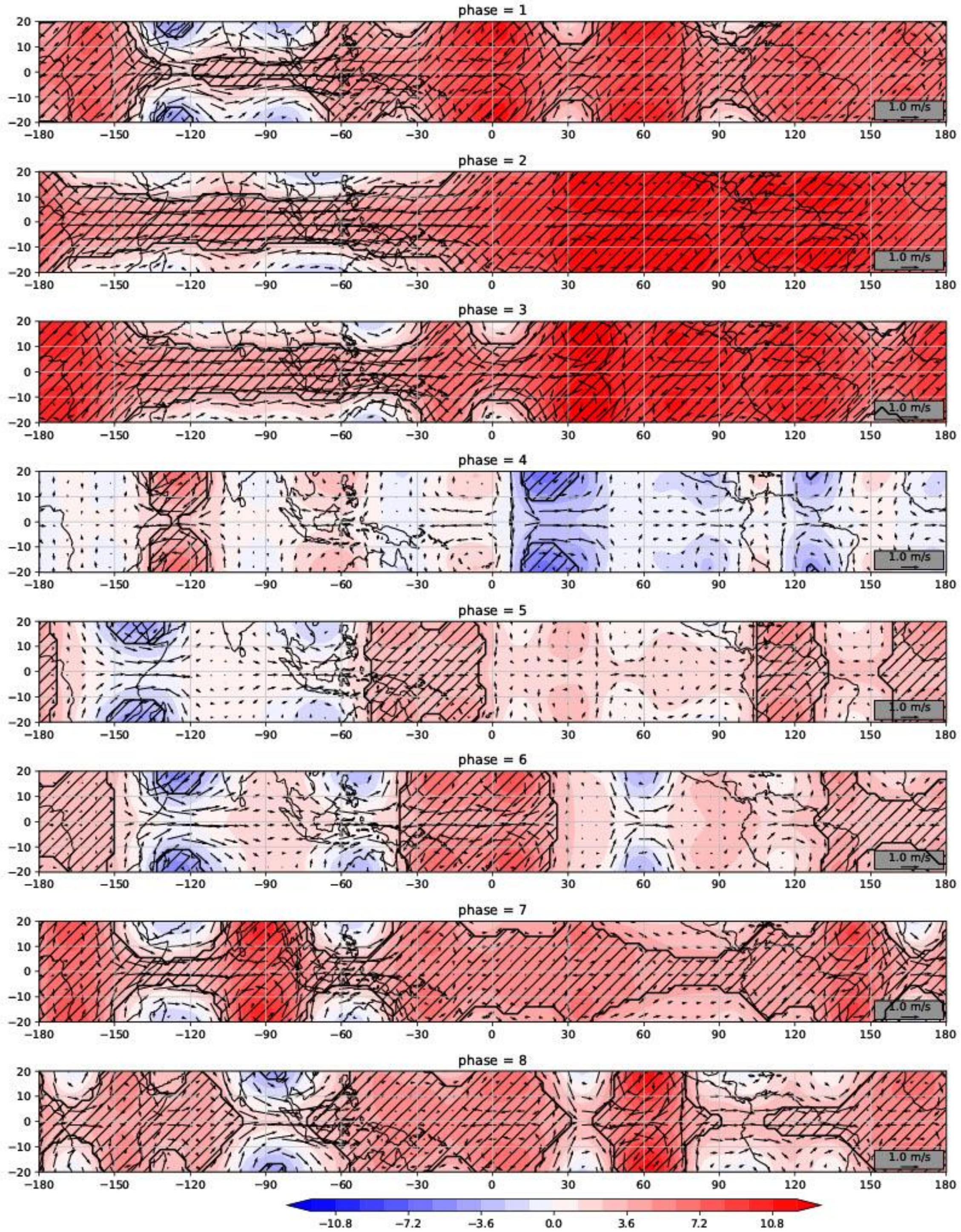

Figure 2.7.4: Difference between of the velocity and geopotential height fields associated with ROT modes with SZW30+ and SZW30-. The hatched region corresponds to significant difference of the geopotential height values under 5% confidence level.

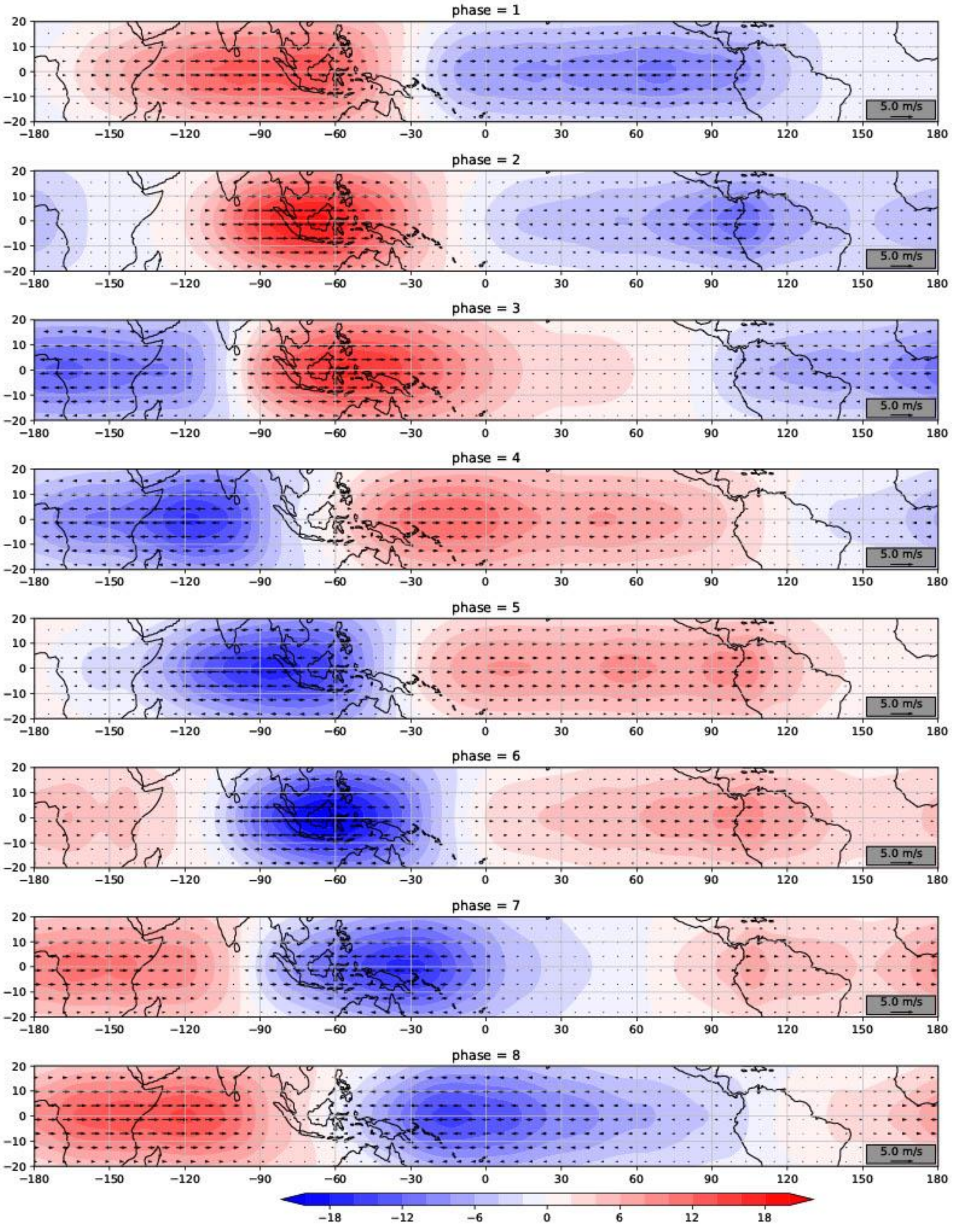

Figure 2.7.5: Reconstruction of the velocity and geopotential height fields associated with Kelvin modes with SZW30+ at 200 Mb.

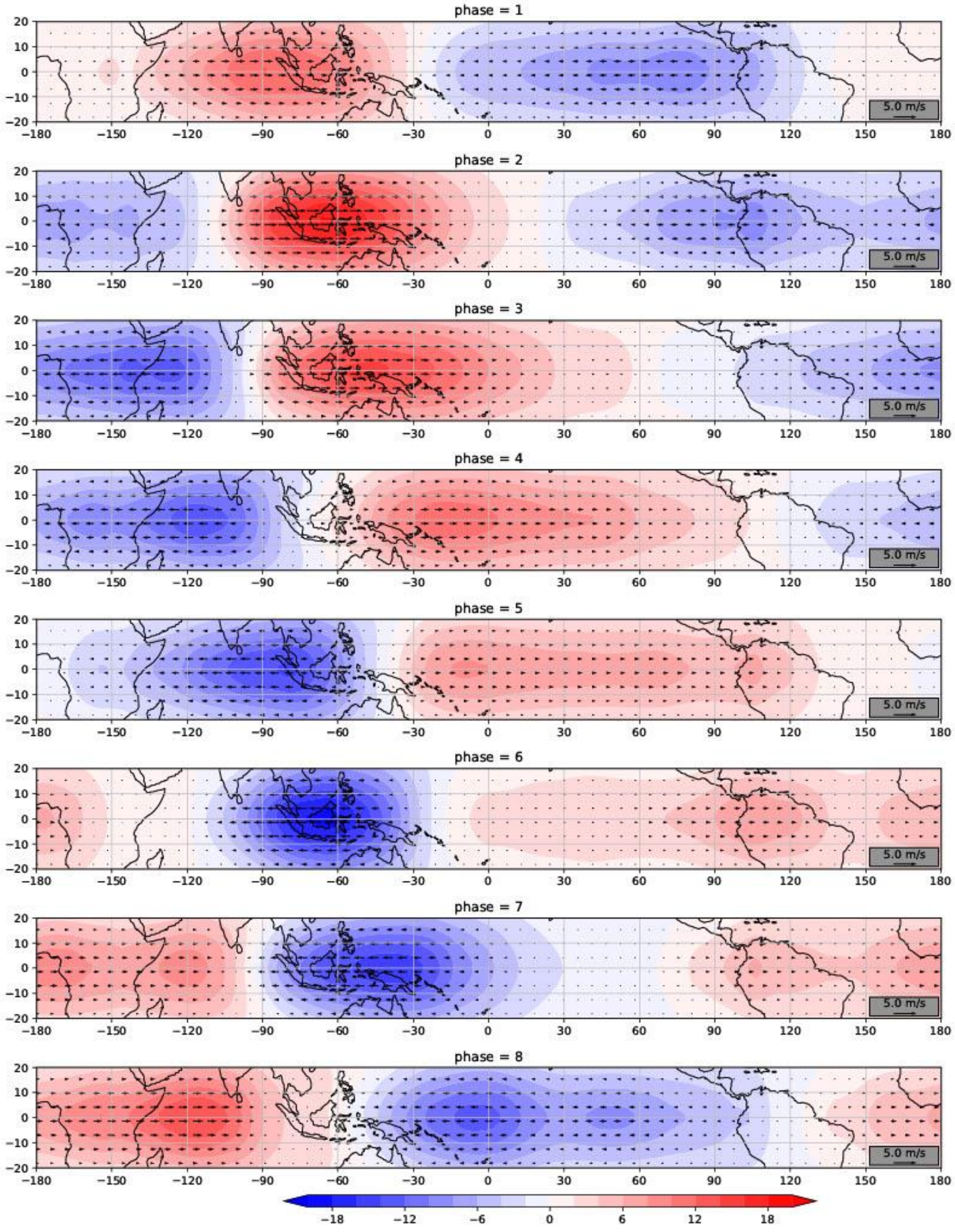

Figure 2.7.6: Reconstruction of the velocity and geopotential height fields associated with Kelvin modes with SZW30- at 200 Mb.

Figures 2.7.5 and 2.7.6 display respectively the composites associated with the reconstructions of velocity and geopotential height fields associated with the Kelvin mode for each of the 8 MJO phases with positive stratospheric zonal wind at 30 mb (SZW30+) and negative (SZW30+). In order to compare both composites we compute the difference between SZW30+ and SZW30- of each field for each MJO phase. This is displayed in figure 2.7.7. We notice that for phases 1-3 the difference (of the geopotential height fields represented by the hatched region) is statistically significant for almost the entire domain. Unlike in the case of ROT modes, for the Kelvin modes the distribution of statistically significant difference is more even throughout a MJO cycle with a larger area on phase 2 and more similar fields on phase 4. It is possible to notice a propagation pattern with negative geopotential height anomaly beginning at phase 4 and ending at phase 7.

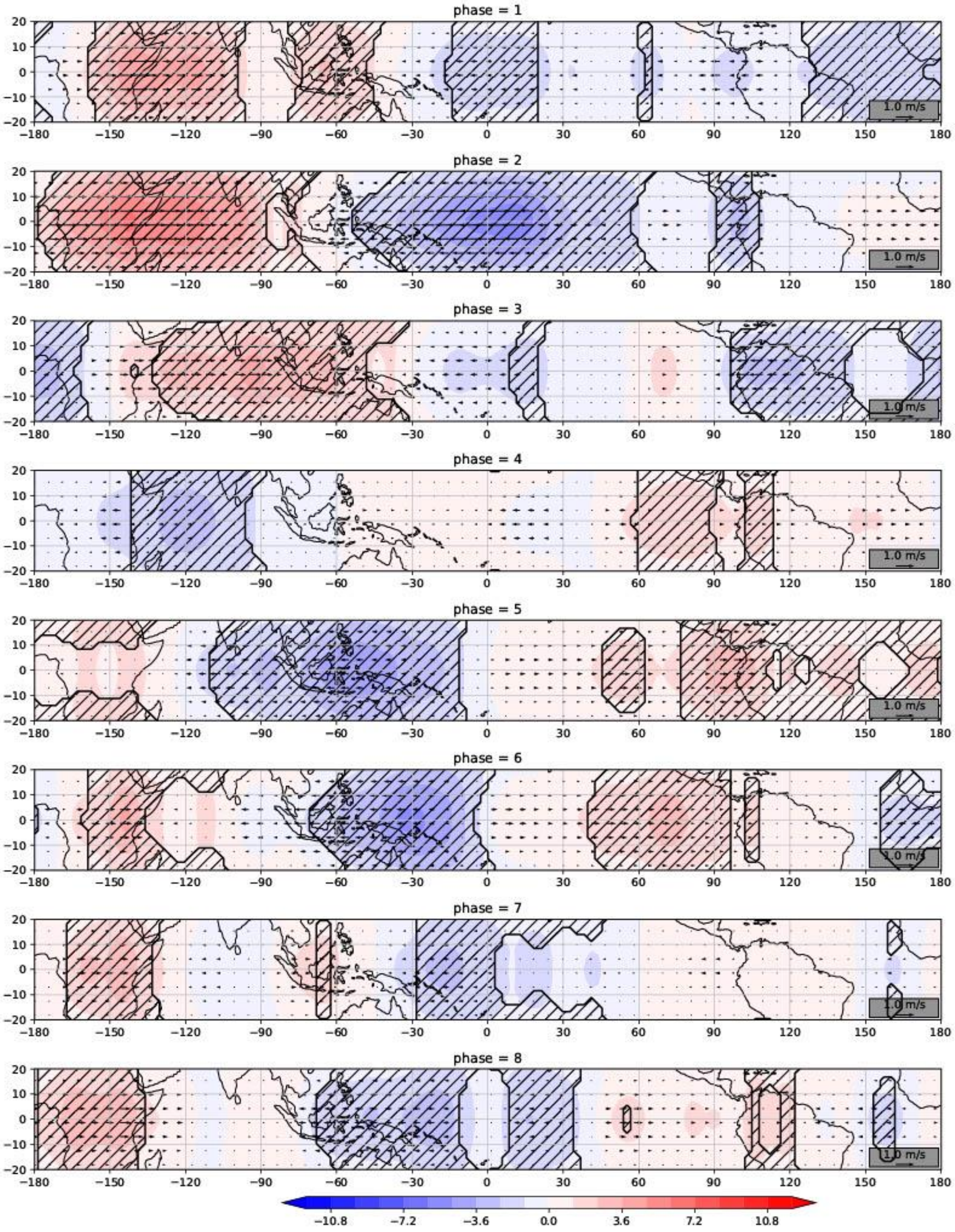

Figure 2.7.7: Difference between of the velocity and geopotential height fields associated with Kelvin modes with SZW30+ and SZW30-. The hatched region corresponds to significant difference of the geopotential height values under 5% confidence level.

8) Please correct “Frankze” to “Franzke” in the references.

The correction was made.

1) The analysis and interpretation of section 3 is suspect (and possibly in other sections). Figure 1 clearly shows regular and artificial peaks at regular (frequency) intervals most likely resulting from the bandpass pre-processing of the data. The features look similar to those which would appear in data convolved with a square filter. I recommend that suitable prefiltering is done to minimise these numerical artefacts (i.e. using appropriate tapering methods).

The reviewer is correct that the signal was rectified to analyze the effect oonly on the amplitude of the time series. Nevertheless, it seems that this procedure created some doubt about the validity of our result. Therefore, we re analyze the data without rectifying the the signal and now report this result. We apologize for this confusion. The new figure is the following.

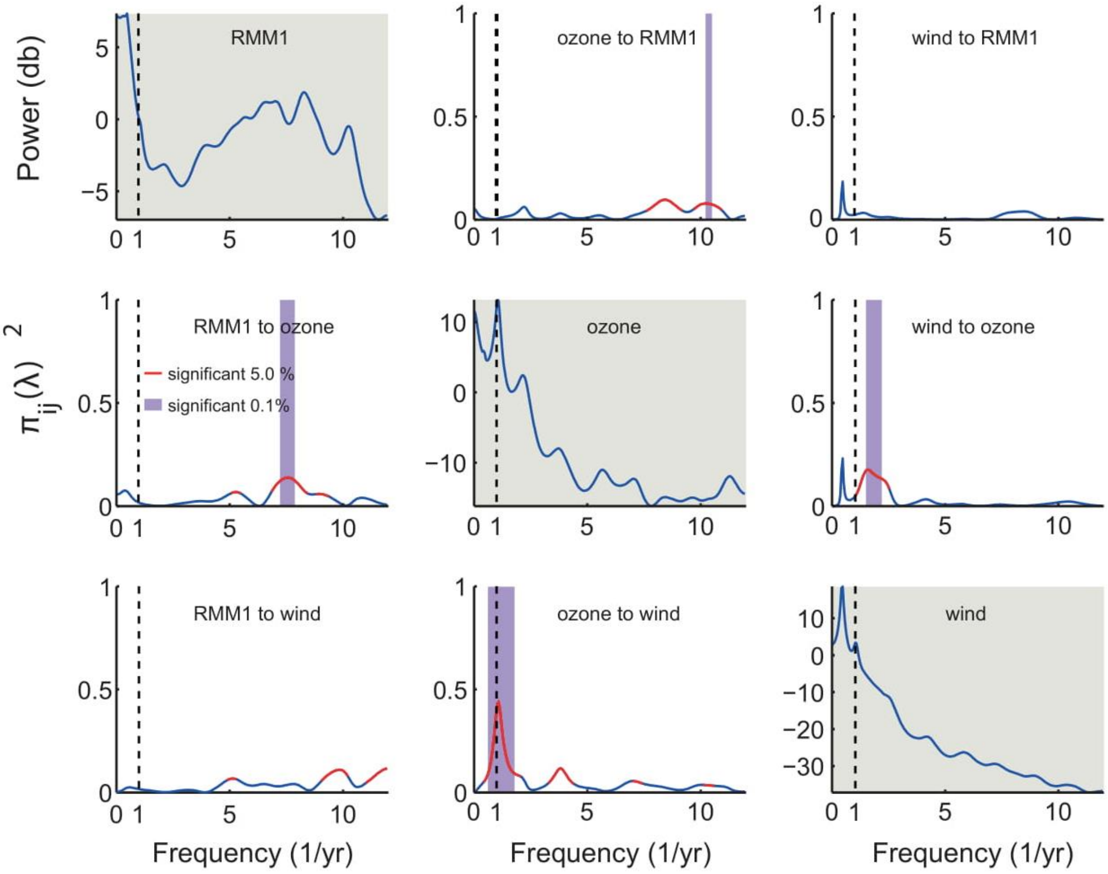

Figure 3.1.1: PDC analysis of the RMM index, QBO and ozone at the fast (intraannual time-scale).

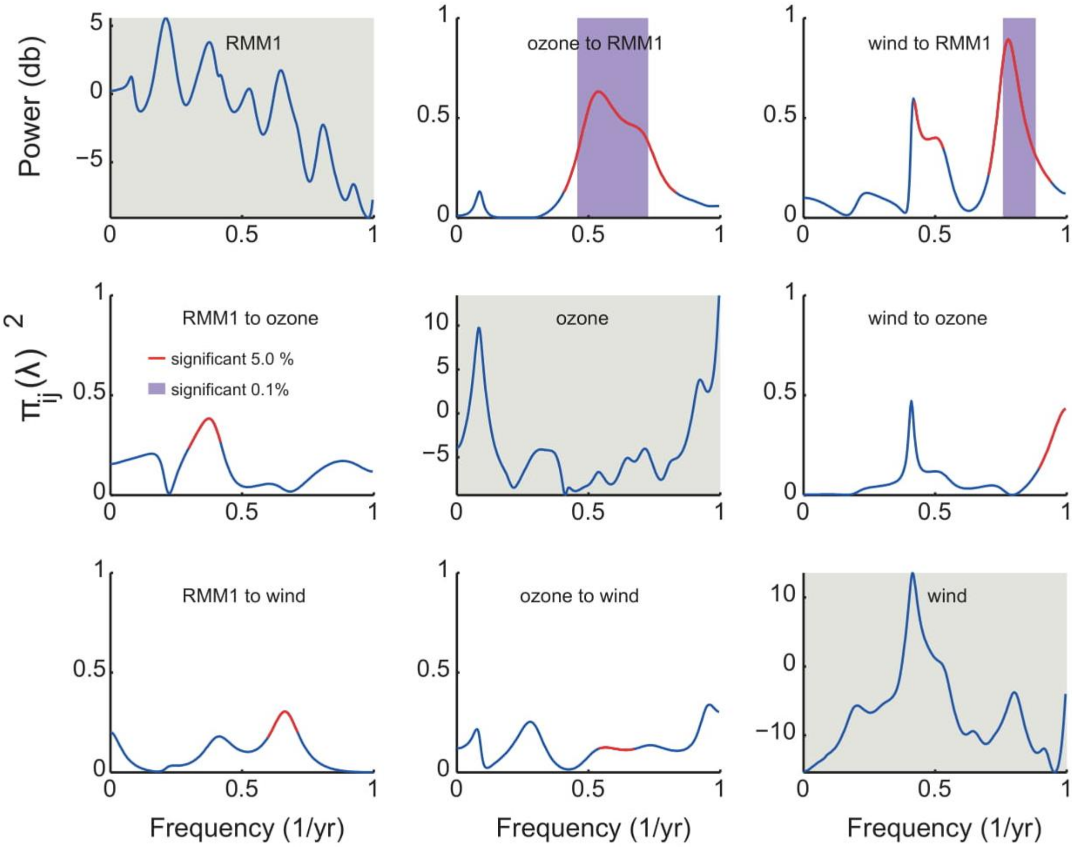

Figure 3.1.2: PDC analysis of the RMM index, QBO and ozone at the slow (inter-annual time-scale).

2) It seems to this reviewer that the annual cycle has been retained in the data. Presumably retention of the annual cycle and sub-harmonics will obscure attribution of causality between the various timeseries? Why has the annual cycle been retained and what impact will this have on the interpretation of the results?

We did not remove the annual cycle. The reviewer is correct to mention that the annual cycle is a dominant component of the all spectra investigated here, this however is not a problem once other spectral peaks of interest (i.e intraseazonal, biennial, interannual and decadal) are well represented by the parametric spectral estimation procedure. As explained in answer to question 7 of this reviewer our ability to well represent the spectral peaks of interest rely on the order of the auto-regressive model of choice.

3) The authors should provide figures for the timeseries used in the paper, before and after processing, including those short and long timeseries used throughout the manuscript.

Here we include a new figure with the corresponding time-series which will be included in the new version of the manuscript.

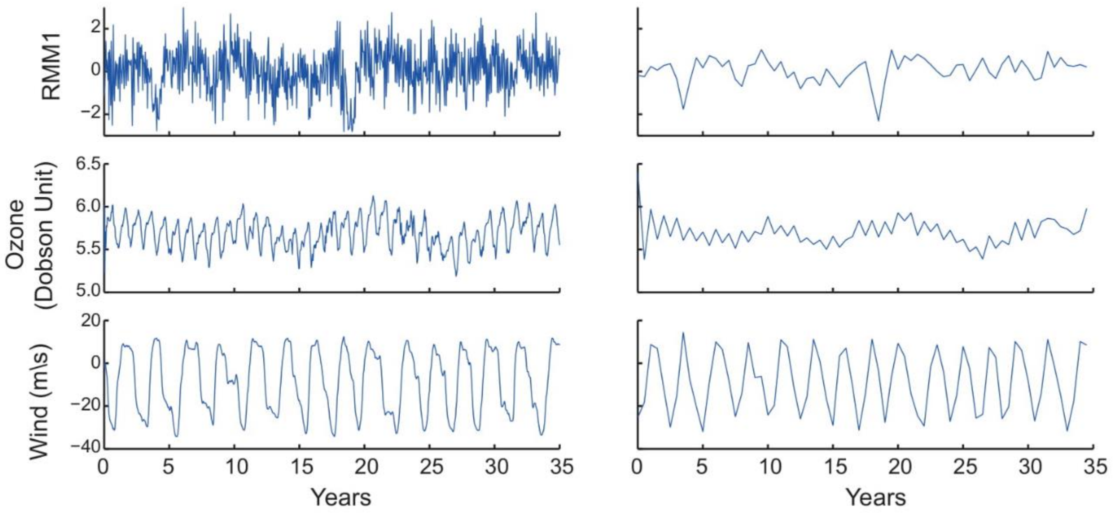

Figure 3.3.3: Time-series of the RMM index, stratospheric zonal wind at 30Mb and equatorial ozone.

4) The authors have not justified the use of indices thought relevant for MJO-QBO connections, namely MJO indices and the westward propagating gravity wave modes (and various others wave modes). There are a number of competing mechanisms for explaining the observed correlations between the MJO and QBO. A number of these do not explicitly involve waves, but rather upper tropospheric temperature, wind-shear or static-stability. The title of the paper suggests a focus on waves, but this needs to naturally come following an appraisal of the various mechanisms first.

The study of QBO effects on the MJO gained a lot of interest in the last few years, since new evidence pointed out to this connection (see Yoo, C., & Son, S. W. (2016). Modulation of the boreal wintertime Madden‐Julian oscillation by the stratospheric quasi‐biennial oscillation. *Geophysical Research Letters*, *43*(3), 1392-1398.). Since then several articles explored both the physical mechanisms behind this interaction as well as consequences to weather and climate. One of the main factors that plays a factor in the QBO-MJO connection is the difference in the static stability at the Tropopause region depending on the phase of the QBO (see Nishimoto, E., & Yoden, S. (2017). Influence of the stratospheric quasi-biennial oscillation on the Madden–Julian oscillation during austral summer. *Journal of the Atmospheric Sciences*, *74*(4), 1105-1125.). Hendon et. al 2018 suggests that negative temperature anomalies at the tropopause region at the eastern QBO act act to destabilize the upper troposphere in phase with MJO associated convection, thus reinforcing the MJO event (see Hendon, H. H., & Abhik, S. (2018). Differences in vertical structure of the Madden‐Julian Oscillation associated with the quasi‐biennial oscillation. *Geophysical Research Letters*, *45*(9), 4419-4428.). Alternative mechanisms that could contribute to this stratosphere-troposphere connection include the downward reflection of planetary waves (see Lu, H., Scaife, A. A., Marshall, G. J., Turner, J., & Gray, L. J. (2017). Downward wave reflection as a mechanism for the stratosphere–troposphere response to the 11-yr solar cycle. *Journal of Climate*, *30*(7), 2395-2414.) and effects on tropospheric Rossby wave-guides and teleconnection patterns (see Feng, P. N., & Lin, H. (2019). Modulation of the MJO-related teleconnections by the QBO. *Journal of Geophysical Research: Atmospheres*, *124*(22), 12022-12033.).

Here we investigate a different class of mechanism, namely the role of wave interaction. Nonlinear wave interaction is believed to have a role in the initiation of an MJO event though the interaction between the tropics and extra-tropics (see section 6.4 of Khouider, B., Majda, A. J., & Stechmann, S. N. (2012). Climate science in the tropics: waves, vortices and PDEs. *Nonlinearity*, *26*(1), R1.). This interaction takes place by by the coupling between equatorially confined modes, the baroblinic Rossby waves, and non-confined modes, the barotropic Roosby waves. Inspired by this type of mechanism we investigate whether the interaction between QBO-related modes with MJO-related modes could have a role in the MJO-QBO connection.

5)The various horizontal/vertical normal modes used to construct QBO and MJO patterns and timeseries need to be captured somewhere (e.g. supplementary materials) as they feature prominently in the analysis.

In our analysis we have used no truncation on the zonal wave- number with K=32 and vertical index up to M=43. The selection of modes is made on the type of the mode (rotational or inertio-gravity). On the meridional index, for the MJO only the first three modes symmetric wind structure with respect to the equator (indices n=1,3,5) were used for the rotational mode and the Kelvin mode (eastward inertia-gravity with meridional index n=1).

6) There is a lot of various missing information on the figures (labels, units, tickmarks etc), which has mostly been identified in the points below. All figures need to be improved for future review.

In the new version of the manuscript we have included corrected versions of the figures.

7) The spectra look very smooth; has any smoothing been applied to the power spectra? If so, how has this been achieved?

Yes, the whole PDC analysis relies on a autoregressive estimation of the spectra, this means that the choice of the autoregressive order will determine the smoothness of the spectra. The lower the chosen model less spectral peaks will be captured by the parametric estimate of the spectra, meaning that only the dominant spectral peaks will be represented, conversely high order models will be able to capture the fine structure of the spectra. In our analysis the order of the autoregressive fitting was in the range 10-15, and were well adjusted according to the Portmanteau test. This means that the resulting spectra will be fairly smooth.

8) Figures 8-11. What physical mechanism will causally link wave modes on interannual to decadal timescales? What hypothesis is being tested?

In our analysis we have calculated the energy time-series associated with normal modes and tested the causality between these energy time-series. We regard this as an evidence for nonlinear wave interaction similar to the barotropic-baroclinic Rossby wave interaction that plays a role in the initiation of the MJO (see Majda, A. J., & Biello, J. A. (2003). The nonlinear interaction of barotropic and equatorial baroclinic Rossby waves. *Journal of the atmospheric sciences, 60*(15), 1809-1821.).

9) Can the authors put forward a plausible physical mechanism linking the Himalayas near 30-40N and two equatorially confined phenomena – MJO and QBO? Furthermore, how should this mediate the observed statistical relationship between the QBO and MJO?

In the present version of the manuscript we have removed this section of the article and replaced it by a composite analysis showing the evolution of each normal mode component of the MJO following the suggestion of Reviewer #2. However, the idea here is that the strong divergence associated with these topographic gravity waves would act as a source of barotropic (in the troposphere) Rossby waves that could interact with the MJO via tropical-extra tropical interaction. We however acknowledge that this is still highly speculative and think that the composite analysis brings much more information on the process.

10) The authors have looked at large scale circulation processes in assessing longtime scale relationships between the QBO and MJO. What though are the roles for small-scale gravity waves in linking QBO and MJO connections?

One of the possible roles of small scale gravity waves is related with their vertical propagation, which is known to be a major mechanism for the QBO, therefore differences on the vertical wave propagation could in principle affect both the QBO and tropical convection (associated with the MJO) (see Piani, C., Durran, D., Alexander, M. J., & Holton, J. R. (2000). A numerical study of three-dimensional gravity waves triggered by deep tropical convection and their role in the dynamics of the QBO. *Journal of the atmospheric sciences*, *57*(22), 3689-3702.).

Stratospheric ozone and QBO interaction with the tropical troposphere on intraseasonal and interannual time-scales: a normal mode perspective

Breno Raphaldini[1], Andre Seiji Watake Teruya[1], Pedro Leite da Silva Dias[1], Daniel Y. Takahashi[2], and Lucas Massaroppe[1]

[1]Department of Atmospheric Sciences, University of Sao Paulo
[2]Instituto do Cerebro,Federal University of Rio Grande do Norte

Correspondence: Breno Raphaldini (brenorfs@gmail.com)

Abstract. The Madden Julian Oscillation (MJO) is the main controller of the weather in the tropics on intraseasonal time-scales and recent research provides evidences that the Quasi-Biennial Oscillation (QBO) influences the MJO interannual variability. However the physical mechanisms behind this interaction are not completely understood. Recent studies on the normal mode structure of the MJO indicates the contribution of global-scale Kelvin and Rossby waves. In this study we test whether these MJO-related normal modes are affected by the QBO and stratospheric ozone. The Partial Directed Coherence method was used and enabled us to probe the direction and frequency of the interactions. It was found that equatorial stratospheric ozone and stratospheric zonal winds are connected with the MJO at periods of 1-2 months and 1.5-2.5 years. We explore the role of normal mode interactions behind the stratosphere-troposphere coupling by performing a linear regression between the MJO/QBO indices and the amplitudes of the normal modes of the atmosphere obtained by projections on a normal mode basis using ERA-Interim reanalysis data. The MJO is dominated by symmetric Rossby modes but is also influenced by Kelvin and asymmetric Rossby modes. The QBO is mostly explained by westward propagating inertio gravity waves and asymmetric Rossby waves. We explore the previous results by identifying interactions between those modes and between the modes and the ozone concentration. In particular, westward inertio-gravity waves, associated with the QBO, influence the MJO on interannual time-scales. MJO related modes such as the Kelvin wave and the Rossby wave with symmetric wind structure with respect with the equator are shown to have significantly different dynamics during MJO event depending on the phase of the QBO.

1 Introduction

The Madden Julian Oscillation (MJO) and the Quasi-Biennial Oscillation (QBO) are two of the main elements of the atmospheric low frequency variability in the tropics. The MJO acts on intraseasonal time-scales on the troposphere and impacts the tropical monsoons and with global impacts (*Zhang*, 2005). The QBO manifests in the tropical stratosphere as a reversal of the zonal winds with descending cycles with mean period of 28 months also with important impacts on the Global circulation of the atmosphere (*Holton & Tan* , 1980). Both are important players for the Earth system's weather and climate. Careful examination of causal relationships between such processes and the physical mechanisms behind their interaction are active topics of research in recent years (*Zhang et. al.*, 2018).

The stratosphere can act as a mediator between solar forcing and the climate variability of the troposphere. It is conjectured that stratospheric influence on the troposphere exists via the so-called top-down mechanism (*Gray et. al.*, 2010). According to this hypothesis, stratospheric ozone absorbs ultraviolet solar (UV) radiation releasing heat. This heat then generates temperature and wind perturbations in the stratosphere that might then induce a tropospheric response through downward energy transport. However, details of the physical mechanisms through which stratospheric signals could propagate down to the troposphere are not completely understood.

Stratospheric control of tropospheric phenomena in mid to high latitudes was addressed in several papers. For instance, *Baldwin et. al.* (2010) highlights the polar vortex as an important example of such control. Another example is that of stratospheric impacts on tropospheric upper level jets and storm tracks as seen in *Kidston et. al.* (2015). *Yoo & Son* (2016) showed that the MJO is sensitive to the QBO phase in the annual timescale, concluding that including QBO information improves the MJO predictability (*Marshall et. al.*, 2017; *Son et. al.*, 2017). *Densmore et. al.* (2019) attributes differences on the QBO-MJO interaction to the QBO phase to differences in the static stability of the upper troposphere/lower stratosphere, leading to changes in the excitation of MJO-related disturbances. *Hendon & Abhik* (2018) associated the increased predictability and intensity of the MJO during the boreal winter and QBO easterly phase with differences in the vertical structure of the MJO, depending on the QBO phase. The problem of MJO-QBO connection is however still not well understood from the perspective of the underlying physical mechanism nor well represented in numerical models as pointed out recently in *Kim et. al.* (2020).

The study of QBO effects on the MJO gained a lot of interest in the last few years, since new evidence pointed out to this connection (*Yoo & Son*, 2016). Since then several articles explored both the physical mechanisms behind this interaction as well as consequences to weather and climate. One of the main factors that plays a factor in the QBO-MJO connection is the difference in the static stability at the Tropopause region depending on the phase of the QBO (). *Hendon & Abhik* (2018) suggests that negative temperature anomalies at the tropopause region at the eastern QBO act act to destabilize the upper troposphere in phase with MJO associated convection, thus reinforcing the MJO event . Alternative mechanisms that could contribute to this stratosphere-troposphere connection include the downward reflection of planetary waves (*Lu et. al*, 2017) and effects on tropospheric Rossby wave-guides and teleconnection patterns (). Here we investigate a different class of mechanism, namely the role of wave interaction. Nonlinear wave interaction is believed to have a role in the initiation of an MJO event though the interaction between the tropics and extra-tropics (see section 6.4 ()). This interaction takes place by by the coupling between equatorially confined modes, the baroblinic Rossby waves, and non-confined modes, the barotropic Rossby waves. Inspired by this type of mechanism we investigate whether the interaction between QBO-related modes with MJO-related modes could have a role in the MJO-QBO connection.

Recent studies have given a normal mode description of the MJO (*Zagar & Franzke*, 2015; *Kitsios et. al.*, 2019). These studies concluded that the MJO can be described as global scale baroclinic Rossby and Kelvin waves. The same approach was used to study the conditions that lead to the 2016 QBO disruption (*Raphaldini et. al.*, 2020). In this context a natural question arises: what is the role of these normal modes in the MJO interaction with the stratosphere? In particular, how do these modes interact with QBO-related modes?

In this article, we study the interactions between the stratosphere and the tropical troposphere, with particular emphasis on the MJO. A time series analysis causality method, Partial Directed Coherence (PDC), (*Baccala & Sameshima*, 2001) was used. We determine whether equatorial ozone, equatorial stratospheric zonal winds and tropospheric fields interact and how this interaction occurs, including information on directional interaction. Our analysis is based on daily data of stratospheric zonal wind, ozone concentration, and the unfiltered (on the intreseasonal timescale) MJO index from 1979 to 2015. We obtained stratospheric zonal wind and ozone concentration from ERA-Interim reanalysis data (*Dee et. al.*, 2011) from the European Centre for Medium-Range Weather Forecasts. Zonal wind at 30 hPa level was averaged in an equatorial belt from -15^o to 15^o latitude for all longitudes, which is a reasonable choice to represent the QBO (*Nappo*, 2013). Ozone data were averaged from -20 to 20 in latitude and integrated over all levels from 100 to $0.1hPa$. MJO data was obtained from the daily MJO index RMM (*Wheeler & Hendon*, 2004). The MJO index is presented in a polar coordinate diagram with two time-series, amplitude and phase. The amplitude of the MJO index is defined as the sum of the squares of the first two empirical orthogonal functions (EOFs) of combined pressure fields at 200 and $850hPa$ and outgoing long wave radiation data in the tropics (RMM1 and RMM2). An equivalent way to represent the MJO index (a complex number) is to use two real variables that correspond to the two first components. In order to use minimal mathematical operations with the original EOF time-series we choose the last representation.

To resolve the spectrum of the different time-scales, time-scale separation was applied to the data. We split the data into a fast time-scale (periods shorter than one year), and a slow time-scale (periods greater than one year). This was done by performing a resampling procedure on the data with a ten-day rate for the "fast" time-scale. A six-month window was applied for the "slow" time-scale.

The causality between the QBO, tropical stratospheric ozone and the MJO, was studied using the PDC method. PDC corresponds, roughly, to a frequency domain counterpart of the Granger Causality test (*Baccala & Sameshima*, 2001), with the additional advantage of providing information on the specific frequencies at which the causality occurs.

We seek for normal modes that might contribute for interactions between stratospheric and tropospheric phenomena by performing a linear regression with the MJO indices and stratospheric zonal winds. We then perform the PDC analysis with the time series for the energies associated with each of the Hough modes responsible for the MJO dynamics (as in *Zagar et. al.* (2015)) and of the stratospheric zonal wind. The results indicate that the interaction of internal westward gravity waves, responsible for the QBO and Kelvin, and Rossby waves associated with the MJO, partially explain the stratospheric influences on the MJO.

2 Methods

2.1 Granger Causality

The concept of causality is a central question in science. One possible definition of causality related to the predictability of two or more distinct processes was introduced in *Granger* (1969) and is currently known as Granger causality in the literature. The main advantage is the ability to pinpoint the direction of interaction, unlike other measures such as coherence, correlation, partial coherence and partial correlation. The following definition is specific to trivariate time series but is readily generalizable to an arbitrary number of time series.

Consider a vector-valued signal $\mathbf{X}(t) = [X_1(t), X_2(t), X_3(t)]^\top$ where the supersprict $^\top$ indicates the transpose of a vector and $\mathbf{X}(t)$ is assumed to have a vector autoregressive representation of order p (hereafter referred as VAR(p))

$$\begin{bmatrix} X_1(t) \\ X_2(t) \\ X_3(t) \end{bmatrix} = \sum_{k=1}^{p} \begin{bmatrix} a_{11}(k) & a_{12}(k) & a_{13}(k) \\ a_{21}(k) & a_{22}(k) & a_{23}(k) \\ a_{31}(k) & a_{32}(k) & a_{33}(k) \end{bmatrix} \begin{bmatrix} X_1(t-k) \\ X_2(t-k) \\ X_3(t-k) \end{bmatrix} + \begin{bmatrix} \epsilon_1(t) \\ \epsilon_2(t) \\ \epsilon_3(t) \end{bmatrix}, \tag{1}$$

where $a_{ij}(k)$ are the VAR(p) coefficients representing the $k-$th lagged influence of the $j-$th component of the signal on the $i-$th component and t denotes the time variable. The innovations processes (the random component) $\epsilon_i(t)$ have zero mean and covariance matrix $\mathbf{C} = [\sigma_{ij}]$, such that $Cov(\epsilon_i(t), \epsilon_j(s)) = 0$ for $t \neq s$ and for all $i, j \in \{1, 2, 3\}$.

It is enough to say that $X_j(t)$ Granger causes $X_i(t)$ for $i \neq j$ if $a_{ij}(k) \neq 0$, with statistical significance, for some lag $k = 1, \ldots, p$. Thus, the absence of Granger causality from $X_1(t)$ to $X_2(t)$ implies that $X_1(t)$ does not help to predict $X_2(t)$, once the past of $X_2(t)$ and $X_3(t)$ are considered.

In practice, given a trivariate time series $\mathbf{X}(t)$ of length n, we estimate the VAR(p) model from the data and test for $a_{ij}(k)$ nullity. More precisely, the idea is verify the null hypothesis

$$\mathcal{H}_0: \; a_{ij}(k) = 0, \; k = 1, \ldots, p, \tag{2}$$

against

$$\mathcal{H}_1: \; \text{there exist } \; k \in \{1, \cdots, p\}, \; \text{such that } \; a_{ij}(k) \neq 0. \tag{3}$$

In summary, we can say that the $j-$th component of the time series causes the $i-$th component in the sense of Granger if the past of the $j-$th component helps to predict the future of the $i-$th component. We have used the MATLAB Toolbox (free) implementation of the VAR(p) and Granger causality estimators implementations from *Sameshima et. al.* (2015), available at http://www.lcs.poli.usp.br/~baccala/pdc.

2.2 Partial directed coherence

Partial Directed Coherence (PDC) is an extension of the concept of Granger causality to the frequency domain, as a measure of information flow. Thus, PDC incorporates advantages of the Granger causality and of the classical coherence methods with the additional advantage that it can be generalized to more than two time series enabling to explicitly pinpoint the directed information flow from mere indirect interactions, (*Baccala & Sameshima*, 2001; *Takahashi et. al.*, 2007, 2010). PDC has been successfully applied in complex systems as neurocience (*Baccala & Sameshima*, 2001; *Schelter et. al.*, 2006) and economics (*Hui & Chen*, 2012). PDC was also used to detect the causality between the El Niño Southern Oscillation and the monsoons and also in the sea-air interaction in the South Atlantic Convergence Zone (*Tribassi et. al*, 2017).

Again, consider a trivariate time series $\mathbf{X}(t) = [X_1(t), X_2(t), X_3(t)]^\top$ with a VAR(p) representation defined in (1), let

$$\bar{A}_{kl}(\nu) = \delta_{kl} - \sum_{s=1}^{p} a_{kl}(s)\mathrm{e}^{-\mathrm{i}2\pi\nu\mathrm{s}}, \tag{4}$$

where δ_{kl} is the Kronecker delta symbol, $\mathrm{i}^2 = -1$, ν the Fourier frequency (in Hertz), s the time (in seconds). Here we use the more general PDC definition, the information-Partial Directed Coherence (${}_i$PDC), which is closely related to information theory. It has been shown that ${}_i$PDC corresponds to the information flow (in Shannon's sense) between different signals (*Baccala et. al.*, 2013). Therefore the information flow, ${}_i$PDC, from $X_j(t)$ to $X_i(t)$ in a specific frequency ν, is given by

$$_i\mathrm{PDC}_{i\leftarrow j}(\nu) = {}_\iota\pi_{ij}(\nu) = \frac{\bar{A}_{ij}(\nu)/\sqrt{\sigma_{ij}}}{\sqrt{\bar{\mathbf{a}}_j^{\mathsf{H}}(\nu)\mathbf{C}^{-1}\bar{\mathbf{a}}_j(\nu)}}, \tag{5}$$

where $\bar{\mathbf{a}}_j(\nu)$ is the $j-$th column of the matrix with coefficients $\bar{A}_{kl}(\nu)$, and $\bar{\mathbf{a}}_j^{\mathsf{H}}(\nu)$ denotes its Hermitian transpose.

Note that there is a duality between the Granger causality and PDC, as demonstrated in *Sameshima et. al.* (2015). Therefore the nullity of ${}_\iota\pi_{ij}(\nu)$ corresponds to the absence of connection (similarly to the aforementioned Granger causality condition), which, in the PDC case, also has a rigorous and well-defined statistical criterion for the null hypothesis test (*Baccala et. al.*, 2013). Confidence intervals for the PDC analysis are explicitly calculated as the statistics of the PDC coefficients, ${}_\iota\pi_{ij}(\nu)$, is asymptotically Gaussian (at the limit of a large number of data points). For a proof of this theorem and more information on confidence intervals for PDC see *Baccala et. al.* (2013) and *Takahashi et. al.* (2007). To estimate the ${}_i$PDC from the data, the first step is to obtain the vector autoregressive model, which is estimated through the Hannan-Quinn criterion in this paper and substitute the estimated coefficients in Eq.(3). The implemented test statistics are described in *Baccala et. al.* (2013), and we used the computations of ${}_i$PDC generated from AsympPDC Package version 3.0 MATLAB Toolbox freely available as mentioned before. A detailed example showing how to interpret the PDC plots is given in the supplementary material (see figure S1).

The partial directed coherence technique as well as Granger causality related techniques are linear in nature and a natural question is whether these technique are able to capture the interaction between signals that arise from nonlinear problems. There are several publications addressing this question such as possible nonlinear extension of this technique (*Massaroppe & Baccala*, 2015; *Wahl et. al.*, 2016) and the introduction of other techniques that are intrinsically nonlinear in nature, based on time lagged embedding, such as *Sugihara et. al.* (2012), or based on the concept of Markov partitions, such as *Bianco-Martinez et. al.* (2018). *Sugihara et. al.* (2012) gives an example in which Granger based techniques perform poorly. Here we argue that although PDC does not capture all kinds of nonlinear coupling between time scales especially with more intermittent/non-Gaussian behavior, it certainly captures certain kinds of nonlinear interactions. As proved in *Takahashi et. al.* (2010) there is an equivalence between the concepts of mutual information rate that would account for all information flow between two or more signals and PDC, in the case of Gaussian processes. In the general non-Gaussian case bounds are given for the difference of the mutual information rate estimated by PDC and the actual mutual information rate, meaning that even if the signals are nonlinear and non-Gaussian PDC is still able to capture part of the information flow between the signals.

The main advantage of PDC and Granger causality is that it is theoretically related to the mutual information rate (MIR) between signals (*Takahashi et. al.*, 2010), (*Geweke*, 1984). Information-theoretic quantities are usually costly to estimate directly from time-series since it relies on the estimation of multi-dimensional probability distributions. As proved in Takahashi et. al 2010, PDC is a Gaussian approximation to the MIR. This means that if the time-series are stationary and Gaussian PDC provides an exact estimate for the MIR, when the time-series are not Gaussian (possibly due to underlying nonlinearities) the PDC will capture part but not all of the information flow between the time-series. There are many "causality" estimation methods in the literature, all of them with some advantages and drawbacks. Among the several causality detection methods the Convergent-Cross Mapping (CCM) method is proposed as a method that is capable to capture couplings in highly-nonlinear settings since it relies phase-space embedding procedures. CCM. However, it comes with a few drawbacks that would require more in-depth investigation before we could apply it in the present setting, namely: (1) CCM is a bi-variate measure. Granger causality and PDC are genuinely multivariate measures. (2) CCM may lead to wrong or misleading results when moderate to high levels of noise are present (see (*Monster*, 2017)). Granger causality and PDC are designed to work for signals with stochasticity. (3) CCM does not have an automated way to decide the optimal lag between time series. Granger causality and PDC are based on autoregessive process in which order estimation is well studied. (4) There are no theoretical guarantees for the statistical properties of CCM. Both PDC and Granger causality are at very well studied measures in which there are thousands of articles applying it and we understand well their statistical properties (*Lutkepohl*, 2005; *Takahashi et. al.*, 2007).

Finally, although PDC is a stochastic linear method, it correctly reconstruct the topology of networks of nonlinear oscillators , see *Winterhalder et. al.* (2007), Moreover, it has been successfully and extensively used to infer information flow in highly nonlinear time-series data in neuroscience (*Bressler & Seth*, 2011). The fact that PDC can detect nonlinear interactions is not difficult to understand, given that linear regression also can see nonlinear interaction unless the nonlinearity is highly non-monotonic.

2.3 PDC statistics

The PDC is a function of the coefficients of vector autoregressive model. Given that the coefficients are asymptotically jointly normally distributed, we can use the delta method (*Serfling*, 1980) to obtain analytically the asymptotic statistics for PDC. After an algebraic computation we can show that PDC at frequency lambda is distributed asymptotically (under the null hypothesis of zero PDC) as the weighted sum of two chi-square with one degree of freedom (*Takahashi et. al.*, 2007)). Therefore, we can use the the asymptotic distribution to calculate the p-value. For details of the derivation, we refer to *Takahashi et. al.* (2010). The significance level used in the article for PDC is the frequency-wise value as it is the standard for frequency domain analysis given the high correlation between the point estimates for neighboring frequencies (*Huybers & Curry*, 2006; *Came*, 2007)).

2.4 Normal mode decomposition

Based on the methodology of *Kasahara & Puri* (1981), *Zagar et. al.* (2015) introduced a software for the projecting atmospheric fields from reanalysis onto the normal modes of the hydrostatic primitive equations on the sphere. For a vector valued function $\mathbf{X} = [u, v, h]^\top$, where $u(\lambda, \phi, z)$ is the zonal velocity field, $v(\lambda, \phi, z)$ is the meridional velocity field, $h(\lambda, \phi, z)$ is the modified geopotential height. A separation of variables is then performed and the state vector $\mathbf{X}$ is represented as a series of horizontal and vertical structure functions, which in discrete form is

$$\mathbf{X}(\lambda, \phi, z) = \sum_{m=1}^{M} \mathbf{S}_m \mathbf{X}_m(\lambda, \phi) G_m(z), \tag{6}$$

where $\mathbf{X}_m$ is the horizontal structure vector function, G_m is the vertical structure function and $\mathbf{S}_m$ is a square matrix defined as

$$\mathbf{S}_m = \begin{bmatrix} \sqrt{gD_m} & 0 & 0 \\ 0 & \sqrt{gD_m} & 0 \\ 0 & 0 & D_m \end{bmatrix},$$

where g is Earth's gravity and D_m equivalent depth of the $m-$th vertical mode. The horizontal fields $\mathbf{X}_m$, on the other hand, are expanded in Hough harmonics as

$$\mathbf{X}_m(\lambda, \phi) = \sum_{n=1}^{N} \sum_{k=-K}^{K} \chi_{m,n,k} \mathbf{H}_{m,n,k}(\lambda, \phi), \tag{7}$$

where $\mathbf{H}_{m,n,k}$ are the eigenfunctions of the Laplace's tidal equation considering zonal periodicity and regularity at the poles as boundary conditions (*Longuet-Higgins & Selwyn*, 1968). The expansion coefficients $\chi_{m,n,k}$ are obtained as

$$\chi_{m,n,k} = \frac{1}{2\pi} \int_0^{2\pi} \int_{-1}^{1} \mathbf{X}_m(\lambda, \phi) \cdot [\mathbf{H}_{m,n,k}(\lambda, \phi)]^* \, \mathrm{d}\mu \mathrm{d}\lambda, \tag{8}$$

with $\mu = \sin(\phi)$ and the superscript * indicates the complex conjugate. Details of the procedures for obtaining the amplitudes $\chi_{m,n,k}$ from the data is described in *Zagar et. al.* (2015). The MODES software then provides the amplitudes $\chi_{m,n,k}$ given input time scales of reanalysis data. *Zagar & Franzke* (2015) proposed a procedure to decompose the MJO into the contributions of each normal mode by performing a linear regression between the MJO time series and the mode-amplitude time series

$$\boldsymbol{\mathcal{R}}_{m,n,k} = \frac{1}{N-1} \sum_{t=1}^{N} \frac{(\chi_{m,n,k}(t) - \mathbf{E}[\chi_{m,n,k}(t)])\,(Y(t) - \mathbf{E}[Y(t)])}{Var\,[Y(t)]} \tag{9}$$

where $\chi_{m,n,k}(t)$ is the Hough expansion coefficient (8) for a time instant t, $Y(t)$ is the MJO index time series and $\mathbf{E}\,[Y(t)]$ and $Var\,[Y(t)]$ are the respective expectation and variance, respectively.

From the time series of the amplitudes of the normal mode functions we compute the energy within a group of modes, consisting of the sum of the squares of their amplitudes weighted by their equivalent depths D_m:

$$E(t) = \frac{1}{2}\sum_{m=M_0}^{\overline{M}} gD_m \sum_{k=0}^{\overline{K}} \sum_{n=N_0}^{\overline{N}} \Big([\mathcal{X}_{kmn}](t)[\mathcal{X}_{kmn}]^*(t) \Big) \tag{10}$$

where $\overline{M} = 43, \overline{K} = 32$ and $\overline{N}$ are wavenumber truncations, throughout the text we select different N to represent different modes (Kelvin, Rossby, westward inertio-gravity...).

3 Statistical analysis: QBO-MJO-Ozone interaction

Time-series of the stratospheric zonal wind at 30 Mb, equatorial ozone concentration in the stratosphere and the RMM index are presented in Figure 1. The autorregressive fitting of the time series were found to be well-represented by the, passing the Portmanteau test (*Lutkepohl*, 2005). The PDC analysis for the fast (interannual) timescale, Figure 2, indicates that there is a statistically significant interaction between the stratospheric mean zonal wind and the MJO and between tropical stratospheric ozone and the MJO, results here are presented only for RMM1 (RMM2 yield similar results). Concerning the influence of the stratospheric variables on the MJO, tropical stratospheric ozone is shown to have a significant causality (in the Granger sense) on the MJO indices, influencing RMM1 during periods of around one month, corresponding to the higher frequency range of a MJO cycle,. The periods when ozone influences RMM1 and RMM2 show, by the definition of Granger Causality, that information on ozone should improve the MJO predictability.

In order to investigate the interaction between the stratospheric variables and the MJO index we performed a $6-$ month re sampling procedure. Results are presented in Fig. 3. Ozone is found to significantly influence the MJO, what can be seen in Figure 2, on the annual time-scale for RMM2, possibly due to the annual cycle, and on the time-scale of $1.6 - 2.1$ years, possibly associated with the QBO. Both RMM indices are found to be significantly affected at frequencies with a peak at 11 years, which is a strong indication of the effect of the solar cycle on the MJO, through ozone, which could explain the solar cycle related monsoon variability (*VanLoon & Meehl*, 2012). Interactions that are significant are found from ozone to the MJO in a period ranging from one to two years, possibly as a combination of effects of the annual cycle and the QBO, corroborating the recent results in the literature (*Marshall et. al.*, 2017; *Son et. al.*, 2017; *Yoo & Son*, 2016).

4 Modal decomposition and wave interactions

Several studies point out to the role of the interaction of waves with different vertical structure in the dynamics of the MJO. For instance, study the interaction of barotropic and baroclinic Rossby waves in the interaction of the tropics and extra-tropics since baropropic waves are not equatorially confined as the baroclinic ones. *Raupp et. al.* (2008) further explores this mechanism in the initiation of the MJO.A Similar mechanism could in principle play a role in stratospheric-tropospheric interactions, with modes with dominant energy in the stratosphere interacting with modes that have more energy in the troposphere. We, therefore, aim to test such a hypothesis.

We initially perform a linear regression analysis between the time series associated with the MJO indices and to the stratospheric zonal wind representative of the QBO, aiming to find which normal modes best represent such oscillations. This analysis was introduced by *Zagar et. al.* (2015) in a normal mode decomposition of the MJO. *Zagar & Franzke* (2015) showed that the dominant modes in the decomposition are the symmetric Rossby mode (with the largest contribution coming from the Rossby mode with meridional index 1, denoted by RSSY1), as well as Kelvin waves (KW). Both Kelvin and Rossby modes have larger regression coefficient for the vertical mode indices 5-9, which have a first baroclinic structure in the troposphere. We performed a similar analysis with the daily time-series of equatorial zonal wind at 30 hPa which is dominated by the QBO. We find that the dominant modes in our regression analysis are westward propagating gravity waves (WIG) and the first asymmetric Rossby modes (meridional index 2, denoted by RWASY1), we refer to (*Raphaldini et. al.*, 2020) for details on the normal mode decomposition of the QBO.

We seek for interactions between the MJO and QBO normal modes. In order to do so, we calculate the time-series of the energy associated with each of the modes (i.e. a weighted sum of the square of absolute value of each of the modes). We begin by describing the interaction between modes associated with the MJO and to the QBO and tropical stratospheric ozone forcing on sub-annual time scales. Due to the large number of variables we split the analysis into three sets, each containing all the "stratospheric variables" against one of the variables associated with the MJO. Since the most important interactions between QBO modes and MJO modes are through the QBO-related WIG waves, we restrict the analysis to these modes.

In 5 we present the PDC analysis of the interaction of Kelvin wave vs. westward inertio-gravity wave vs. stratospheric ozone vs. asymmetric Rossby wave, the first three variables associated with stratospheric phenomena and the last one associated with the MJO. We observe that the ozone forcing acts directly on the MJO related Kelvin waves, most notably on intraseasonal time-scales, with a peak around 50 days. The influence of ozone on this mode is also relevant on a semi-annual and annual time-scale both associated to the annual cycle. WIG waves are found to influence the Kelvin waves on the time-scale of 30 days, while asymmetric Rossby waves are found to influence the Kelvin waves on time-scales from around 50 days to the semi-annual and annual time-scales. We find a feedback from the Kelvin wave to the stratospheric-related variables on intraseasonal, semi-annual and annual time-scales.

Finally, we perform the PDC analysis of the interaction between symmetric Rossby wave (the dominant mode on the MJO decomposition), asymmetric Rossby wave,WIG wave and stratospheric ozone on the fast time-scale. The corresponding PDC plot is presented in 4. The influence of stratospheric ozone on symmetric Rossby waves has peaks at 40 days, 60 days and on a semi-annual time-scale. The influence of the modes associated to the stratospheric zonal wind on the MJO-related Rossby mode seems to be significant throughout the entire intraseasonal time-scale range, most notably around $30 - 40$ days, as well as on semi-annual and annual time-scales. Similarly to the previous cases, the feedback of the MJO-related mode to the stratospheric-related variables takes place on intraseasonal, semi-annual and annual time-scales.

We proceed by analyzing the PDC between the modes associated with stratospheric zonal wind and stratospheric ozone vs MJO-related modes on slow time-scales (annual-decadal time-scales). Most importantly, we search for stratospheric influences on MJO on decadal and biennial time-scales. The analysis of the interaction between Kelvin waves, associated with the MJO and tropical stratospheric ozone is presented in Fig.6. It shows that there is a significant causality from ozone to Kelvin waves on a decadal time-scale. Given that both spectra have a peak on the decadal time-scale we can say that the ozone, which is directly influenced by the solar variability, has a peak directly associated with the solar-cycle and the peak on the Kelvin wave spectrum is at least partially explained by the influence of the ozone on it. Kelvin waves on the other hand influence the ozone on annual time-scales, probably due to the annual cycle. The analysis of the interaction between gravity waves associated with the stratospheric zonal wind and the MJO-related Kelvin waves is presented in Fig. 7. We found an important influence of the westward inertio-gravity waves on the Kelvin waves on biennial time-scales and on decadal time-scales. The first one is clearly associated with the biennial peak on the inertio-gravity wave spectrum which is a product of the quasi-biennial oscillation and might be associated to the results of *Yoo & Son* (2016) and subsequent articles on the relationship between the QBO and the MJO. The PDC peak on the decadal time-scale is possibly associated with the solar cycle and the gravity modes are forced by the ozone 9. Since we do not find spectral peaks on this range, we suspect that this is related to the nearest peak, which is annual. A strong causality is also found on a decadal time-scale, again probably due to the solar cycle. The influence of WIG modes on the MJO related Rossby modes is presented in 8, showing a influence of WIG modes on Rossby modes on annual and biennial timescales.

4.1 Evolution of MJO normal modes

Previous studies point out to different MJO behaviour depending on the phase of the QBO (east or west) (*Yoo & Son*, 2016), it is therefore important to examine how and if these differences manifest on the MJO-related normal modes. In order to do so we follow the methodology used in to study Northern hemisphere extra-tropical response of the MJO using normal mode decomposition. We construct composites presenting velocity and pressure fields associated to MJO-normal modes for each phase of the MJO. In order to exclude periods without MJO events we include in our analysis only days in which $(RMM_1^2 + RMM_2^2 > 1)$. We then divide the MJO events in 8 phases depending on the phase of the MJO $\phi = arctg(RMM_2/RMM1)$. For which QBO (positive or negative) state and for which MJO phase (i=1,2,. . . ,8) we calculated the mean velocity and pressure fields associated with ROT and Kelvin modes at 200 Mb.

Figures 10 and 11 display, respectively, the composites associated with the reconstructions of velocity and geopotential height fields associated with ROT modes for each of the 8 MJO phases with positive stratospheric zonal wind at 30 mb (SZW30+) and negative (SZW30+). In order to compare both composites we compute the difference between SZW30+ and SZW30- of each field for each MJO phase. This is displayed in figure 12. We notice that for phases 1-3 the difference (of the geopotential height fields represented by the hatched region) is statistically significant for almost the entire domain. For phase 4 the fields are more similar with small regions with significant difference, associated with Rossby double vortices. Between phases 5-8 the areas with significant difference become larger again.

Figures 13 and 14 display respectively the composites associated with the reconstructions of velocity and geopotential height fields associated with the Kelvin mode for each of the 8 MJO phases with positive stratospheric zonal wind at 30 mb (SZW30+) and negative (SZW30+). In order to compare both composites we compute the difference between SZW30+ and SZW30- of each field for each MJO phase. This is displayed in figure 15. We notice that for phases 1-3 the difference (of the geopotential height fields represented by the hatched region) is statistically significant for almost the entire domain. Unlike in the case of

ROT modes, for the Kelvin modes the distribution of statistically significant difference is more even throughout a MJO cycle with a larger area on phase 2 and more similar fields on phase 4. It is possible to notice a propagation pattern with negative geopotential height anomaly beginning at phase 4 and ending at phase 7.

5 Final remarks

The PDC results show strong coupling between tropical ozone, stratospheric zonal wind and the MJO. Most notable are the effects of tropical stratospheric winds and ozone influencing the MJO on both intra- and interannual time-scales. The PDC analysis shows that the tropical stratospheric ozone influences the MJO in periods of $30-60$ days and $1.5-2.5$ years. The first period agrees with the MJO period range, suggesting that stratospheric ozone may play a role in the MJO dynamics. The second roughly agrees with the QBO period and the third suggests a solar cycle influence on the MJO. Stratospheric zonal winds also influence the MJO during periods that fall into the QBO period range, in agreement with the recent results of *Yoo & Son* (2016), who showed that there is an interannual variability in the MJO amplitude that depends on the QBO phase. Marshall (2016) also shows that the QBO explains up to 40% of the MJO interannual variability in the boreal winter (also see *Son et. al.* (2017)).

By the definition of Granger causality, one signal causes a second signal if the information of the first helps to predict the future of the other, after taking into account the past of the second signal. In this sense, we confirm the results of the recent studies cited above. We also show that tropical stratospheric ozone also improves the MJO predictability on interannual and decadal time-scales. The periods of interaction suggest that the QBO might be an important process in troposphere/stratosphere coupling through MJO. This conclusion agrees with numerical studies such as that of *Meehl et. al.* (2009), stressing the importance of a realistic QBO in coupled troposphere-stratosphere models. We note that ozone influences the MJO on the intraseasonal time-scales, raising the possibility of tropical stratospheric ozone fluctuations contributing to the initiation of the MJO cycle. On the decadal time-scale, ozone and QBO are modulated by solar activity and ozone was shown to have important impacts on the MJO in this time-scale. There is strong evidence in the literature for the solar cycle impact on the Asian monsoons from both instrumental observations and palaeoclimatic reconstruction, with the rainfall rate in the Indian subcontinent increasing by up to 20% during the solar maximum (*VanLoon & Meehl*, 2012). Since monsoons are linked to the MJO, especially in the Indian region where the MJO signal is strongest, it would be natural to hypothesize that the MJO is a mediator between solar variability and monsoons.

It was also found that the MJO can affect stratospheric ozone, a possible mechanism for this being the impact of deep convection on the tropopause height (*Tian et. al.*, 2007). Another interesting question is whether the relationship between the MJO and the QBO is affected by the recent anomalous behavior of the QBO (*Osprey et. al.*, 2016; *Raphaldini et. al.*, 2020).

As for physical mechanisms that could link stratospheric heating, driven by solar UV forcing, and tropical convection, investigation on tropopause changes caused by ozone absorption is a possible candidate. *Kang et. al.* (2011) suggested a polar latitudes mechanism associated with changes of wave momentum flux due to ozone depletion associated with the ozone hole. Although this mechanism was proposed for high latitudes, it would be interesting to investigate whether it can be extended to the tropics and to ozone changes due to the annual and solar cycles. Recently, *Lu et. al* (2017) suggested that changes in the wave-guides of planetary waves in the stratosphere, caused by solar forcing changes in the mean flow of the stratosphere, might cause downward planetary wave reflection in high solar activity conditions.

We performed a linear regression analysis of the MJO-index and stratospheric zonal winds against the time-series of the amplitudes of the Hough modes. We confirm that the MJO is explained mainly by the first symmetric Rossby Mode (meridional index 1), Kelvin modes, in agreement with *Zagar & Franzke* (2015). The stratospheric zonal wind variability is explained mainly by the WIG modes and the first asymmetric Rossby modes (meridional index 2). We analyzed the interaction among those variables and tropical stratospheric ozone. The exchange of energy between the modes and their interaction with the ozone forcing explains the previous results. We highlight the strong influence of the ozone on the MJO-related modes on the intraseasonal time scale and on decadal time-scales, the last one being possibly a result of the solar cycle. We found influences of the gravity modes on the MJO-related modes to be the most relevant on bi-annual time-scales. This explains at least partially the work of *Yoo & Son* (2016) as well as subsequent articles on the QBO-MJO relation.

Composite analysis of the velocity and geopotential height of the Kelvin and Rossby modes associated with the MJO reveal how the differences in the characteristics of these modes during MJO events when the winds are positive in 30 Mb and when they are negative. For the Rossby modes differences (Fig. 12) are shown to be more significant during initial (1-3) and final (7-8) phases of a MJO cycle, and the spatial pattern is that expected of the rotational component of the MJO with double vortex pattern. The differences reveal a stronger rotational component of the MJO when the zonal winds at 30 Mb are positive. For Kelvin modes significant differences are found throughout the whole MJO cycle and the composite for the difference between the fields from both QBO phases follow a propagation pattern that seem to evolve eastward with similar speed of a typical MJO event (5m/s). This suggests that the QBO effect on the Kelvin mode is more uniform though-out a QBO cycle and in the Rossby modes this effect takes place in the initial and final phases of the MJO.

Code availability. TEXT

Data availability. TEXT

Author contributions. B.R. proposed the study, wrote the manuscript and did the statistical analysis, D.Y.T and L.M. worked on the PDC analysis, A.S.T. performed the normal mode decomposition analysis, P.L.S.D. helped with the discussion and the interpretation of the analysis.

Competing interests. The authors declare that they have no conflict of interest.

Disclaimer. TEXT

Acknowledgements. This work was financed by the FAPESP-PACMEDY project (grants 2015/50686-1 and 2017/23417-5) and CAPES IAG/USP PROEX (grant 0531/2017).

References

Amos, D.E. ; Koopmans, L.H., Tables of the distribution of the coefficient of coherence for stationary bivariate Gaussian processes, Sandia Corporation, 1963.

Baccala, L.A., Sameshima, K. Overcoming the limitations of correlation analysis for many simultaneously processed neural structures. Prog. Brain Res. 130, 33-47 (2001).

Baccala L, De Brito C, Takahashi D, Sameshima K, Unified asymptotic theory for all partial directed coherence forms. Philos Trans R Soc A 371:1–13, 2013.

Baldwin MP, Gillett NP, Forster P, Gerber EP, Hegglin MI, Karpechko AY, Kim J, Kushner PJ, Morgenstern OH, Reichler T. (2010) Effects of the Stratosphere on the Troposphere (Chapter 10), WMO/ICSU/IOC World Climate Research Programme. *World Climate Research Programme.* ,

BIANCO-MARTINEZ, Ezequiel; BAPTISTA, Murilo S. Space-time nature of causality. Chaos: An Interdisciplinary Journal of Nonlinear Science, v. 28, n. 7, p. 075509, 2018.

Bressler, S. L., & Seth, A. K. (2011). Wiener–Granger causality: a well established methodology. Neuroimage, 58(2), 323-329.

Came, R. E., Oppo, D. W., & McManus, J. F. (2007). Amplitude and timing of temperature and salinity variability in the subpolar North Atlantic over the past 10 ky. Geology, 35(4), 315-318.

Dee, D. P., et al. , The ERA-Interim reanalysis: configuration and performance of the data assimilation system, Q. J. R. Meteorol. Soc., 137(656), 553 - 597,2011.

Densmore, Casey R.; Sanabia, Elizabeth R.; Barrett, Bradford S. QBO influence on MJO amplitude over the Maritime Continent: Physical mechanisms and seasonality. Monthly Weather Review, v. 147, n. 1, p. 389-406, 2019.

Diallo, M., Riese, M., Birner, T., Konopka, P., Müller, R., Hegglin, M. I., ... & Ploeger, F. (2018). Response of stratospheric water vapor and ozone to the unusual timing of El Niño and the QBO disruption in 2015–2016. Atmospheric Chemistry and Physics, 18(17), 13055-13073.

Feldstein, S. B. and Lee, S., 2014: Intraseasonal and Interdecadal Jet Shifts in the Northern Hemisphere: The Role of Warm Pool Tropical Convection and Sea Ice. J. Climate, 27, 6497 6518.

Feng, P. N., & Lin, H. (2019). Modulation of the MJO-related teleconnections by the QBO. Journal of Geophysical Research: Atmospheres, 124(22), 12022-12033.

Franzke, C. L., Jelic, D., Lee, S., & Feldstein, S. B. (2019). Systematic decomposition of the MJO and its Northern Hemispheric extratropical response into Rossby and inertio-gravity components. Quarterly Journal of the Royal Meteorological Society, 145(720), 1147-1164.

Freitas, A. C. V. ; Aimola , L. ; Ambrizzi, T. ; de Oliveira, C. P. . Changes in intensity of the regional Hadley cell in Indian Ocean and its impacts on surrounding regions, v. 43, p. 1245-1253, 2016.

Kretschmer, M., Cohen, J., Matthias, V., Runge, J., & Coumou, D. (2018). The different stratospheric influence on cold-extremes in Eurasia and North America. npj Climate and Atmospheric Science, 1(1), 44.

Garfinkel, C. I., and D. L. Hartmann, 2011: The influence of the quasi-biennial oscillation on the troposphere in wintertime in a hierarchy of models. Part I: Simplified dry GCMs. J. Atmos. Sci., 68, 1273–1289.

Geweke, J. F. (1984). Measures of conditional linear dependence and feedback between time series Journal of the American Statistical Association, 79(388), 907-915.).

Granger, C.W.J. Investigating causal relations by econometric models and cross-spectralmethods, 37, 424-438 (1969) 648–650. *Econometrica*

Gray, L. J., Beer, J., Geller, M., Haigh, J. D., Lockwood, M.,Matthes, K., Cubasch, U., Fleitmann, D., Harrison, G., Hood,L., Luterbacher, J., Meehl, G. A., Shindell, D., Van Geel, B., and White, W.: Solar influence on climate, Rev. Geophys., 2010.

Haigh, J. D., and M. Blackburn (2006), Solar influences on dynamical coupling between the stratosphere and troposphere, Space Sci. Rev., 125, 331–344 ,

Hendon, Harry H.; Abhik, S. Differences in Vertical Structure of the Madden-Julian Oscillation Associated With the Quasi-Biennial Oscillation. Geophysical Research Letters, v. 45, n. 9, p. 4419-4428, 2018.

Holton, J. R., & Tan, H. C. (1980). The influence of the equatorial quasi-biennial oscillation on the global circulation at 50 mb. Journal of the Atmospheric Sciences, 37(10), 2200-2208.

Hui, E. C.,Chen, J. (2012). Investigating the change of causality in emerging property markets during the financial tsunami. Physica A: Statistical Mechanics and its Applications, 391(15), 3951-3962. *Physica A: Statistical Mechanics and its Applications.*

Huybers, P., & Curry, W. (2006). Links between annual, Milankovitch and continuum temperature variability. Nature, 441(7091), 329-332.

S. M. Kang, . Polvani,L. M , Fyfe,J.C. Sigmond, M., Impact of Polar Ozone Depletion on Subtropical Precipitation, Science 332, 951 (2011).

KASAHARA, Akira; Puri, Kamal. Spectral representation of three-dimensional global data by expansion in normal mode functions. Monthly Weather Review, v. 109, n. 1, p. 37-51, 1981.

Kidston, J., A. A. Scaife, S. C. Hardiman, D. M. Mitchell, N. Butchart, M. P. Baldwin, and L. J. Gray (2015), Stratospheric influence on tropospheric jet streams, storm tracks and surface weather, Nat. Geosci., 8(6), 433–440, doi:10.1038/ngeo2424.

Khouider, B., Majda, A. J., & Stechmann, S. N. (2012). Climate science in the tropics: waves, vortices and PDEs. Nonlinearity, 26(1), R1.

Kim, H., Caron, J. M., Richter, J. H., & Simpson, I. R. (2020). The lack of QBO-MJO connection in CMIP6 models. Geophysical Research Letters, e2020GL087295.

Kitsios, V., O'kane, T. J., & Žagar, N. (2019). A Reduced-Order Representation of the Madden–Julian Oscillation Based on Reanalyzed Normal Mode Coherences. Journal of the Atmospheric Sciences, 76(8), 2463-2480.

Li, K.-F., Tian, B., Waliser, D. E., Schwartz, M. J., Neu, J. L., Worden, J. R., and Yung, Y. L.: Vertical structure of MJO-related subtropical ozone variations from MLS, TES, and SHADOZdata, Atmos. Chem. Phys., 12, 425-436, 2012.

LIU, Yuyun et al. Three Eurasian teleconnection patterns: Spatial structures, temporal variability, and associated winter climate anomalies. Climate dynamics, v. 42, n. 11-12, p. 2817-2839, 2014.

Longuet-Higgins, Michael Selwyn. The eigenfunctions of Laplace's tidal equation over a sphere. Philosophical Transactions of the Royal Society of London. Series A, Mathematical and Physical Sciences, v. 262, n. 1132, p. 511-607, 1968.

Lu, H., Scaife, A. A., Marshall, G. J., Turner, J., & Gray, L. J. (2017). Downward Wave Reflection as a Mechanism for the Stratosphere–Troposphere Response to the 11-Yr Solar Cycle. Journal of Climate, 30(7), 2395-2414.

Lutkepohl, H. New Introduction to Multiple Time Series Analysis. *(Springer, Berlin,2005).*

Meehl, G. A., J. M. Arblaster, K. Matthes, F. Sassi, and H. vanLoon (2009), Amplifying the Pacific climate system response to a small 11-year solar cycle forcing, Science, 325, 1114–1118,

Majda, A. J., & Biello, J. A. (2003). The nonlinear interaction of barotropic and equatorial baroclinic Rossby waves. Journal of the atmospheric sciences, 60(15), 1809-1821.

Massaroppe, Lucas; Baccala, Luiz A. Detecting nonlinear Granger causality via the kernelization of partial directed coherence. Rio de Janeiro, RJ: ISI-International Statistical Institute, 2015.

Massaroppe, Lucas; Baccala, Luiz A. Kernel-nonlinear-PDC extends Partial Directed Coherence to detecting nonlinear causal coupling. In: 2015 37th Annual International Conference of the IEEE Engineering in Medicine and Biology Society (EMBC). IEEE, 2015. p. 2864-2867.

Marshall, A.G. Hedon, H.H. Hendon Son, S-W Lim,Y. Impact of the quasi-biennial oscillation on predictability of the Madden–Julian oscillation, Clim Dyn (2016).

Monster, D., Fusaroli, R., Tylén, K., Roepstorff, A., & Sherson, J. F. (2017). Causal inference from noisy time-series data—Testing the Convergent Cross-Mapping algorithm in the presence of noise and external influence. Future Generation Computer Systems, 73, 52-62.

NAPPO, Carmen J. An introduction to atmospheric gravity waves. Academic press, 2013.

Nishimoto, E., & Yoden, S. (2017). Influence of the stratospheric quasi-biennial oscillation on the Madden–Julian oscillation during austral summer. Journal of the Atmospheric Sciences, 74(4), 1105-1125.

Osprey, S. M., N. Butchart, J. R. Knight, A. A. Scaife, K. Hamilton, J. A. Anstey, V. Schenzinger, and C. Zhang, An unexpected disruption of the atmospheric quasi-biennial oscillation, 2016. *Science*

Percival, D.B. and Walden , A.T. Spectral Analysis for Physical Applications: Multitaper and Conventional Univariate Techniques. (Cambridge University Press, Cambridge, 1993). *23*

Raphaldini, B., Teruya, A. S., Silva Dias, P. L., Mayta, V.R. C., Takara, V.J. (2020), Normal mode perspective on the 2016 QBO disruption:1evidence for a basic state regime transition , Geophysical Research Letters (In press).

Raupp, C. F., Silva Dias, P. L., Tabak, E. G., & Milewski, P. (2008). Resonant wave interactions in the equatorial waveguide. Journal of the Atmospheric Sciences, 65(11), 3398-3418.

Schelter, B., Winterhalder, M., Eichler, M., Peifer, M., Hellwig, B., Guschlbauer, B., Timmer, J. (2006). Testing for directed influences among neural signals using partial directed coherence. Journal of neuroscience methods, 152(1), 210-219.

Sameshima, K., Baccala, L. A. (1999). Using partial directed coherence to describe neuronal ensemble interactions. Journal of neuroscience methods, 94(1), 93-103.

SAMESHIMA, K.; TAKAHASHI, D. Y. ; BACCALÁ, L. A. . On the statistical performance of Granger-causal connectivity estimators. Brain Informatics, v. 2, p. 119-133, 2015.

Serfling, R. J. (1980). Approximation Theorems of Mathematical Statistics, John Wiley and Sons, New York.

Singh, S. V.; KRIPALANI, R. H.; SIKKA, D. R. Interannual variability of the Madden-Julian oscillations in Indian summer monsoon rainfall. Journal of Climate, v. 5, n. 9, p. 973-978, 1992.

SUGIHARA, George et al. Detecting causality in complex ecosystems. science, v. 338, n. 6106, p. 496-500, 2012.

Son, S.-W., Y. Lim, C. Yoo, H. H. Hendon, and J. Kim(2017): Stratospheric control of Madden-Julian Oscillation, Journal of Climate, 30, 1909-1922.

Takahashi, D.Y., Baccala, L.A. , Sameshima, K. Connectivity inference between neural structures via partial directed coherence. . 10, 1259-1273 (2007). *J. Appl. Stat.* ,

Takahashi, Daniel Y.; Baccalá, Luiz A. ; Sameshima, Koichi . Information theoretic interpretation of frequency domain connectivity measures. Biological Cybernetics v. 103, p. 463-469, 2010.. *Biological cybernetics* ,

Tirabassi, G., Sommerlade, L. and Masoller, C. Inferring directed climatic interactions with renormalized partial directed coherence and directed partial correlation Chaos 27, 035815 (2017).

Tian, B., Yung, Y., Waliser, D., Tyranowski, T., Kuai, L., Fetzer, E., and Irion, F.: Intraseasonal variations of the tropical total ozone and their connection to the Madden-Julian Oscillation, Geophys. Res. Lett., 34, L08704, doi:10.1029/2007GL029451, 2007.

van Loon, H., and G. A. Meehl (2012), The Indian summer monsoon during peaks in the 11 year sunspot cycle, Geophys. Res. Lett., 39, L13701

Tirabassi, G., Sommerlade, L., & Masoller, C. (2017). Inferring directed climatic interactions with renormalized partial directed coherence and directed partial correlation. Chaos: An Interdisciplinary Journal of Nonlinear Science, 27(3), 035815.

Wheeler, M.C. and Hendon, H. H., An All-Season Real-Time Multivariate MJO Index: Development of an Index for Monitoring and Prediction. Mon. Wea. Rev., 132, 1917-1932, 2004.

Yoo, C., and S.-W. Son (2016),Modulation of the boreal winter time Madden-Julian oscillation by thestratospheric quasi-biennial oscillation, Geophys. Res. Lett., 43, *Geophys. Res. Lett.*

Wahl, Benjamin et al. Granger-causality maps of diffusion processes. Physical Review E, v. 93, n. 2, p. 022213, 2016.

Winterhalder, M., Schelter, B., & Timmer, J. (2007). Detecting coupling directions in multivariate oscillatory systems. International Journal of Bifurcation and Chaos, 17(10), 3735-3739.

Žagar, N. et al. Normal-mode function representation of global 3-D data sets: open-access software for the atmospheric research community. Geoscientific Model Development, v. 8, n. 4, p. 1169-1195, 2015.

Žagar, N., & Franzke, C. L. (2015). Systematic decomposition of the Madden-Julian Oscillation into balanced and inertio-gravity components. Geophysical Research Letters, 42(16), 6829-6835.

Zhang, Chidong. Madden-julian oscillation. Reviews of Geophysics, v. 43, n. 2, 2005.

ZHANG, Chidong; ZHANG, Bosong. QBO-MJO Connection. Journal of Geophysical Research: Atmospheres, v. 123, n. 6, p. 2957-2967, 2018.

ZHANG, Taotao et al. The weakening relationship between Eurasian spring snow cover and Indian summer monsoon rainfall. Science advances, v. 5, n. 3, p. eaau8932, 2019.

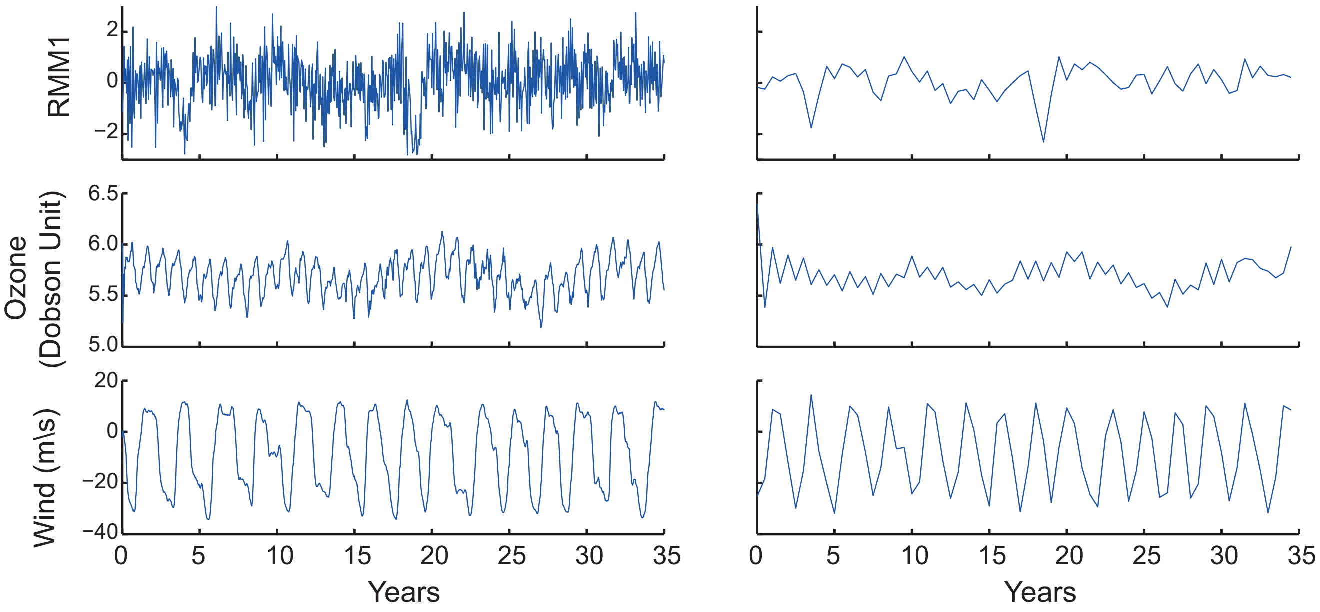

Figure 1. On the left the time series resampled at a 10 days rate of the first component of the MJO index (top), ozone spacially averaged in the equatorial region (middle), and equatorial stratospheric wind (bottom). On the left the same with band with resampling rate of 6 months.

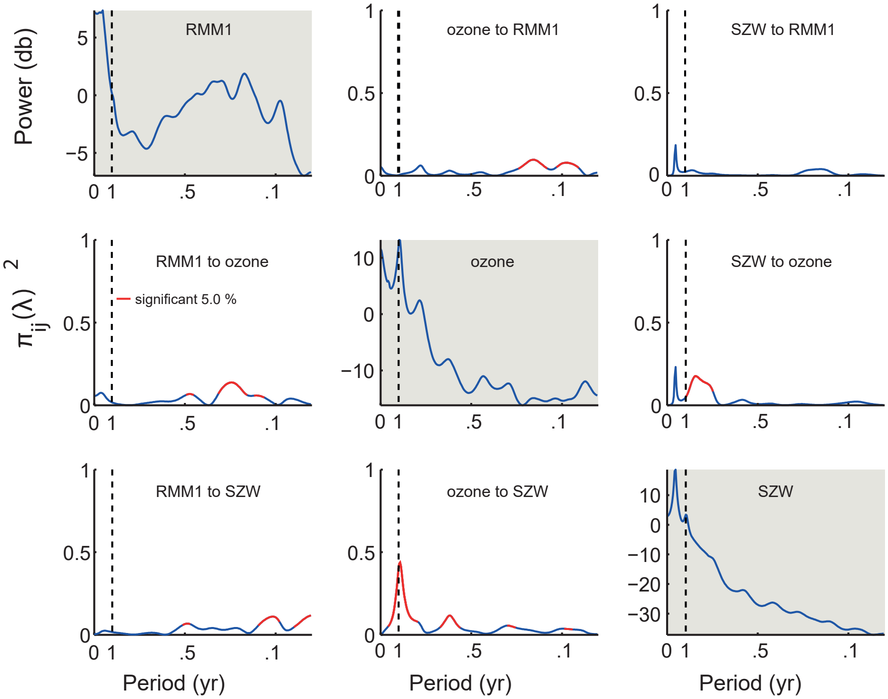

Figure 2. PDC between tropical stratospheric ozone and stratospheric zonal wind (SZW) and the RMM MJO index at the fast (>20days) timescale, frequencies are given are given in cycles/year.

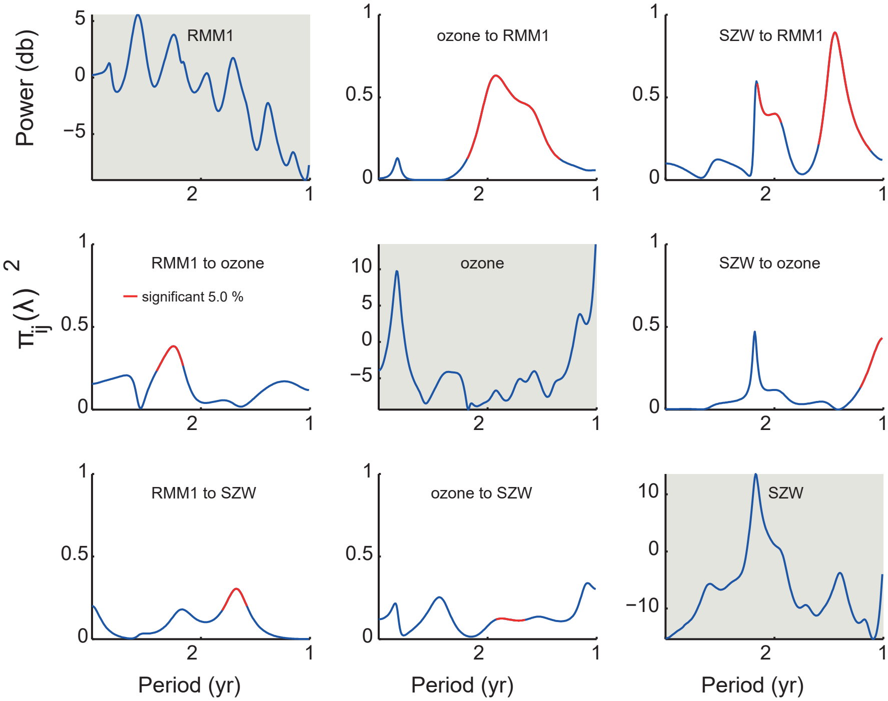

Figure 3. PDC analysis between MJO and Stratospheric zonal winds (SZW) at the slow (>1 year periods) timescale. Results indicate significant interaction on the annual-biennial timescales.

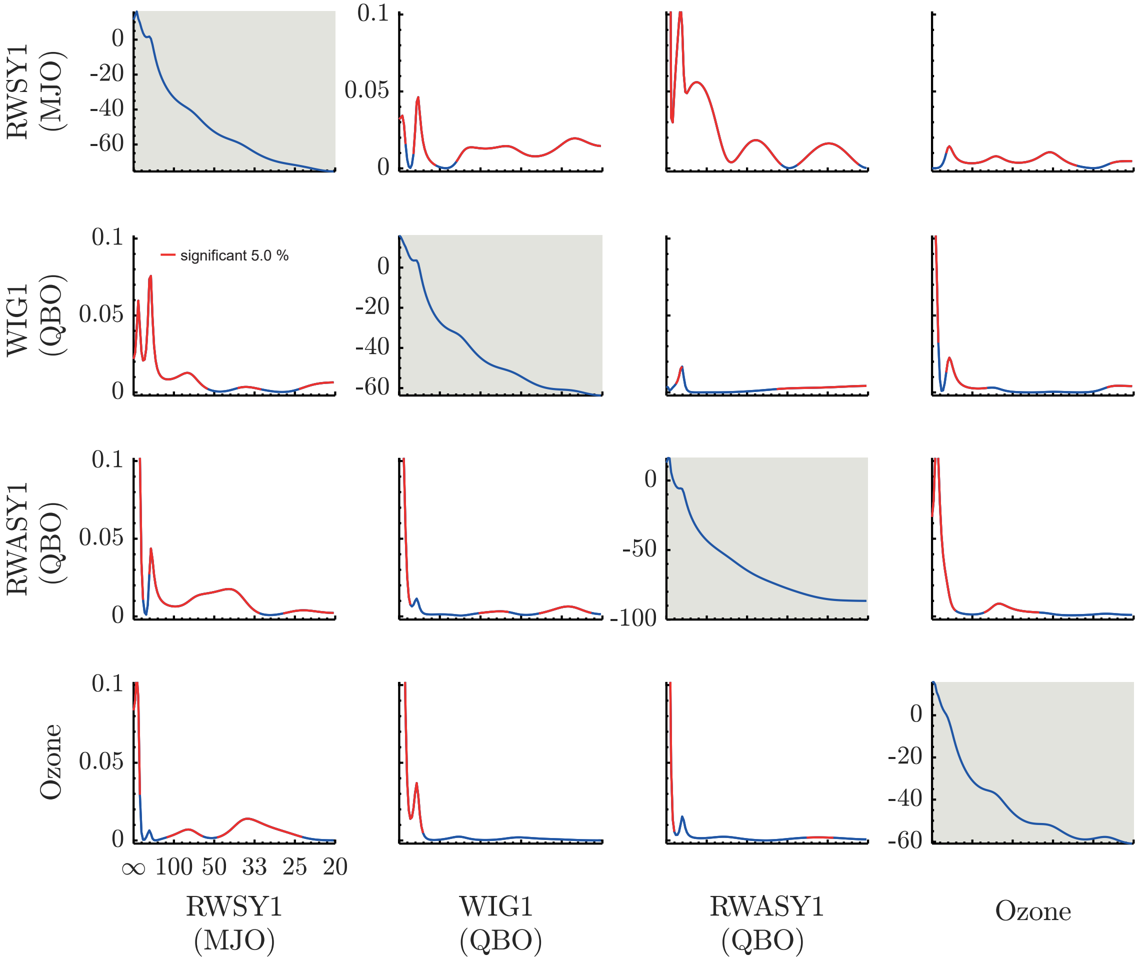

Figure 4. PDC analysis of the interaction of Kelvin, asymmetric Rossby, westward gravity modes and ozone at the fast timescale(periods given in days). Significant interactions (red curve) between MJO and ozone/QBO-related modes is found on intraseasonal, semi-annual and annual time-scales.

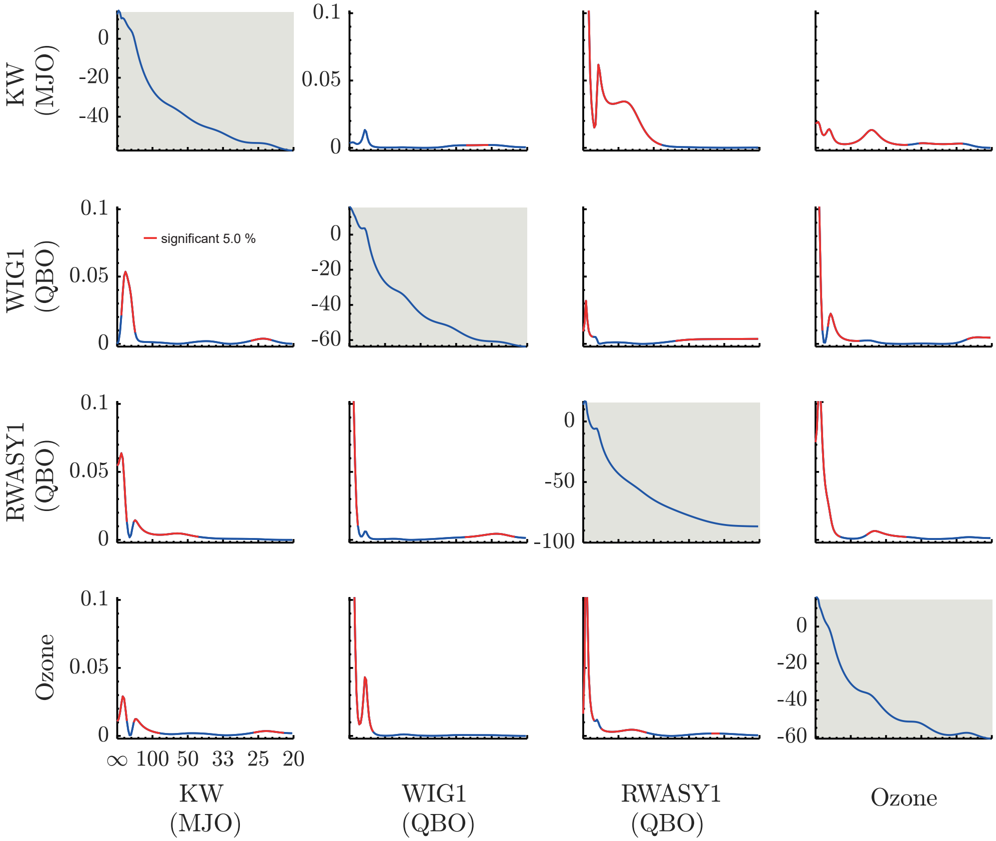

Figure 5. PDC analysis of the interaction of symmetric Rossby n=1, asymmetric Rossby n=1 and westward gravity modes and ozone at the fast timescale (periods given in days). Again, significant interactions (red curve) between MJO and ozone/QBO-related modes is found on intraseasonal, semi-annual and annual time-scales.

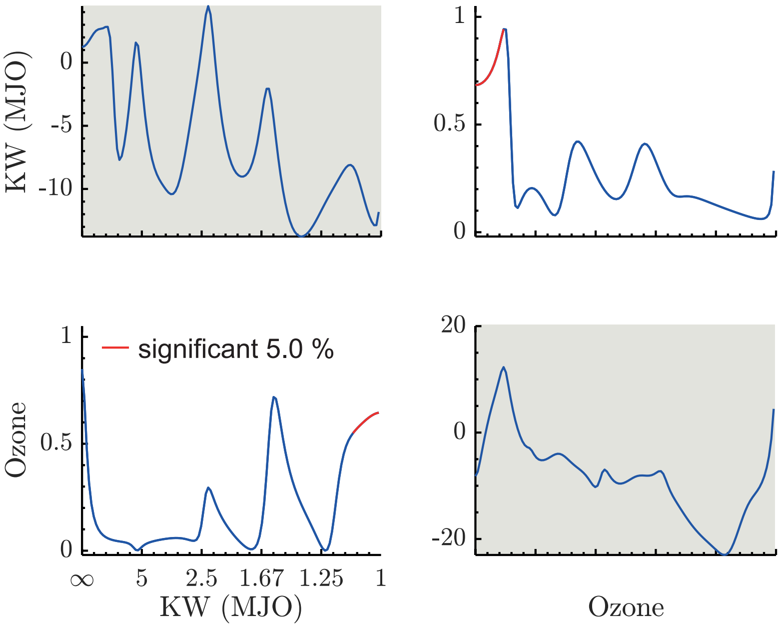

Figure 6. PDC analysis of the interaction of ozone modes and Kelvin waves (KW) at the slow timescale (periods given in years). The results show that KW influence the ozone on the annual time-scale, while the ozone influences KW on decadal time-scales.

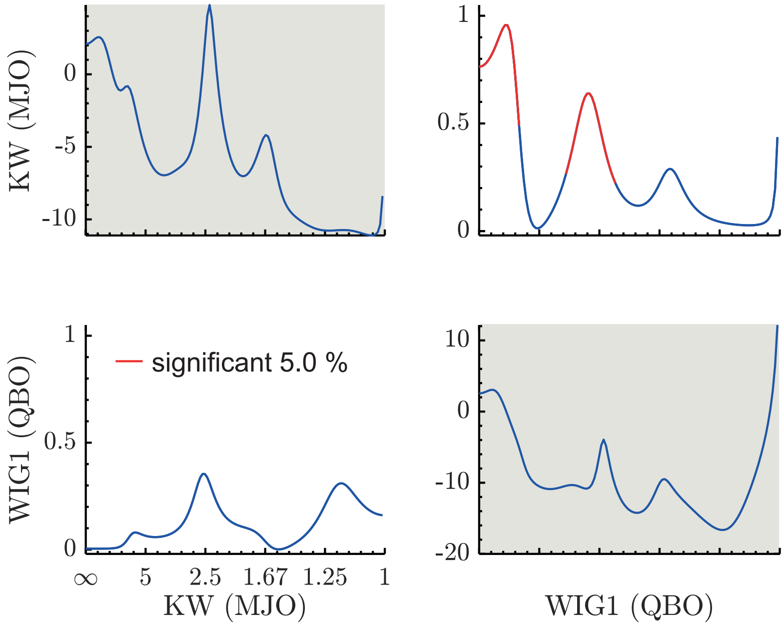

Figure 7. PDC analysis of the interaction of Kelvin modes (KW) and westward gravity modes (WIG) at the slow timescale (periods given in years). The results show a strong influence of the WIG mode on the KW on biennial and decadal timescales.

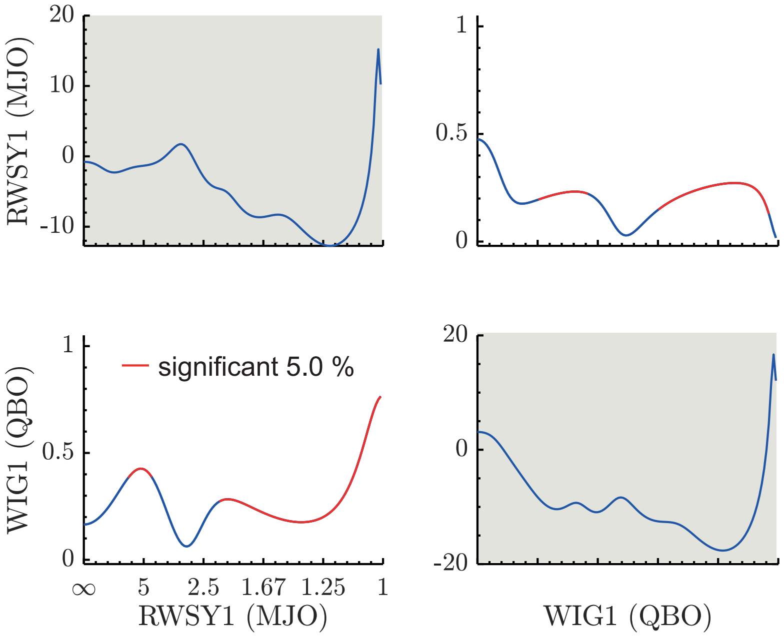

Figure 8. PDC analysis of the interaction of symmetric Rossby modes (meridional index 1, denoted by RWSY1) and westward gravity modes (WIG1) at the slow timescale (periods given in years). Important interactions are found in annual to interannual time-scales.

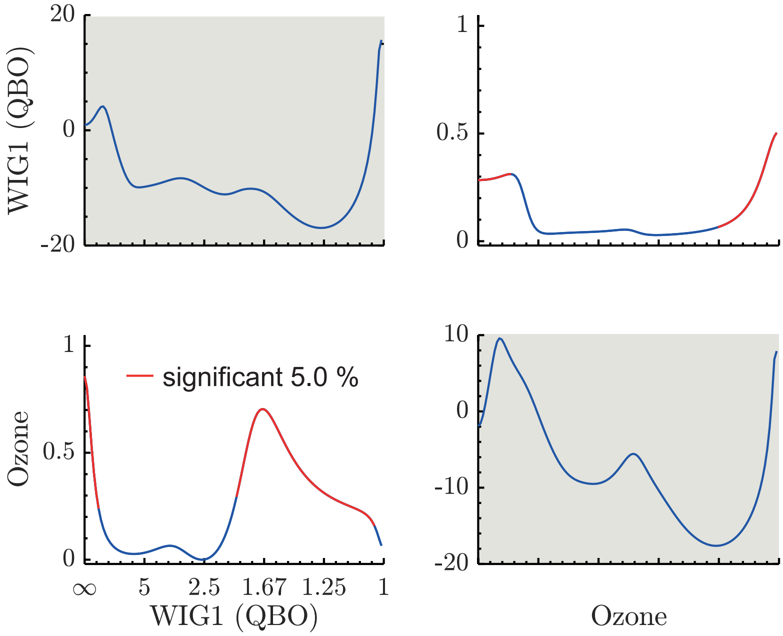

Figure 9. PDC analysis of the interaction of westward gravity modes and ozone at the slow timescale (periods given in years). Important interactions are found on annual-biennial time-scales as well as on the decadal time-scale.

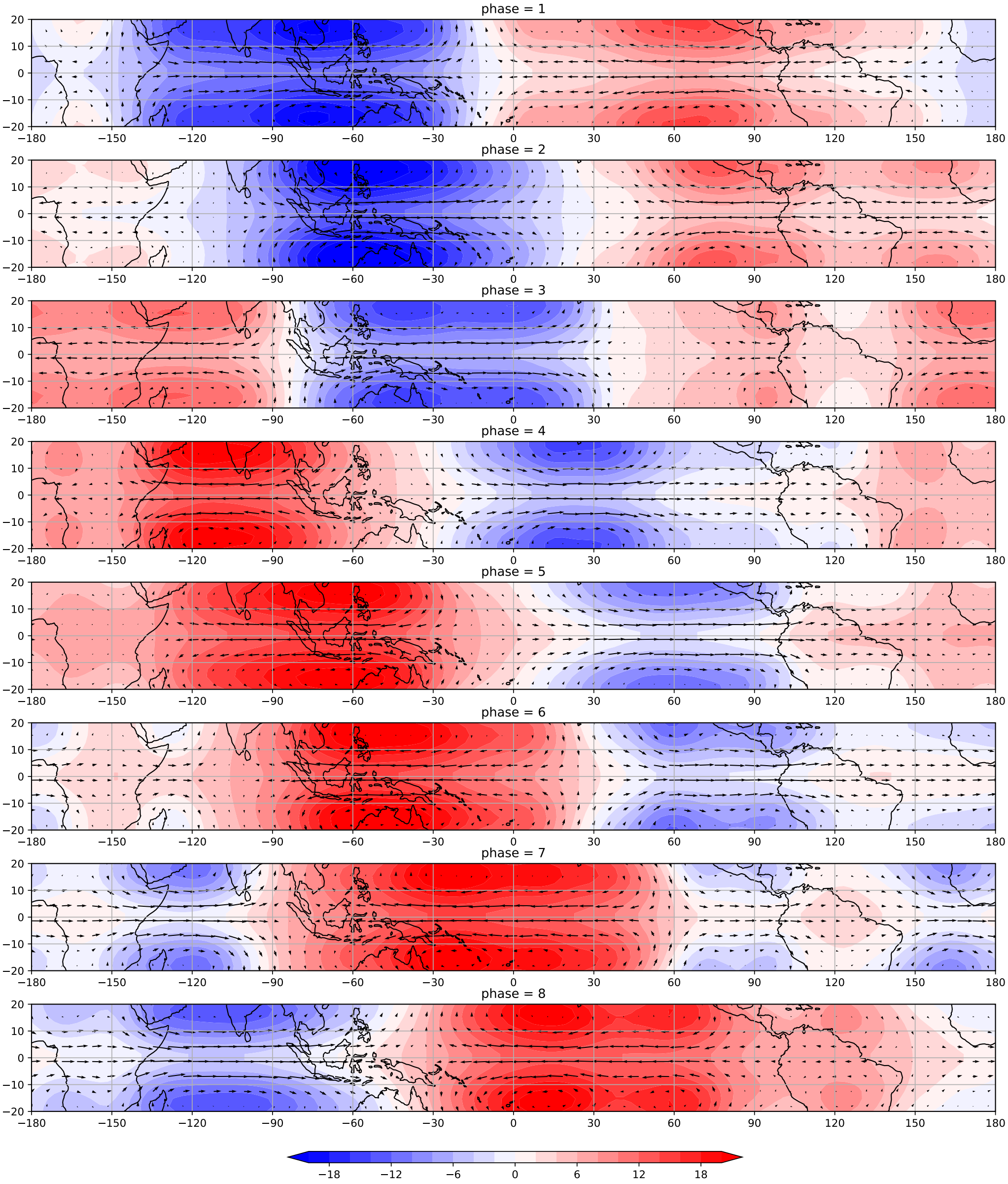

Figure 10. Reconstruction of the velocity and geopotential height fields associated with ROT modes with SZW30+ at 200 Mb.

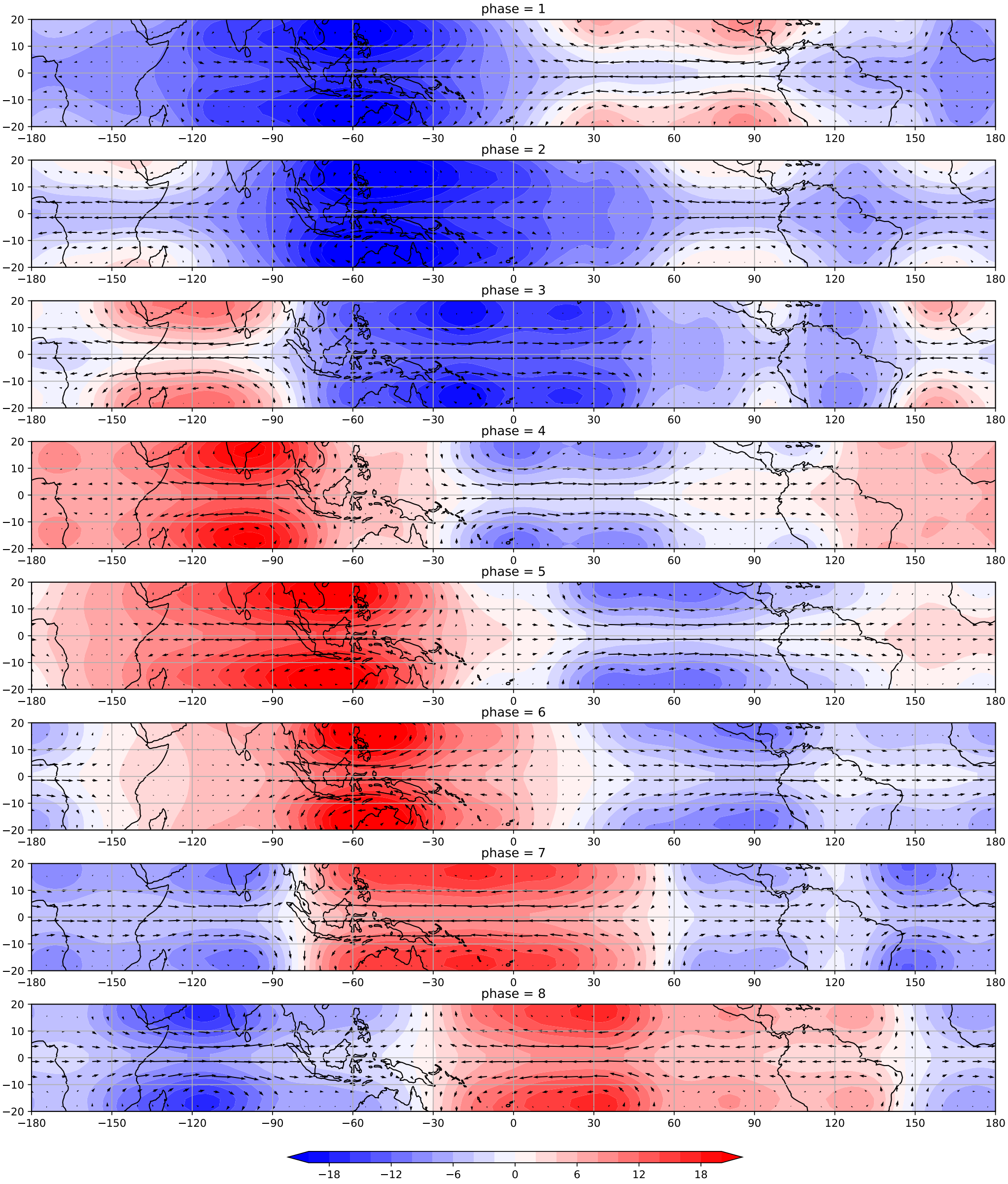

Figure 11. Reconstruction of the velocity and geopotential height fields associated with ROT modes with SZW30- at 200 Mb.

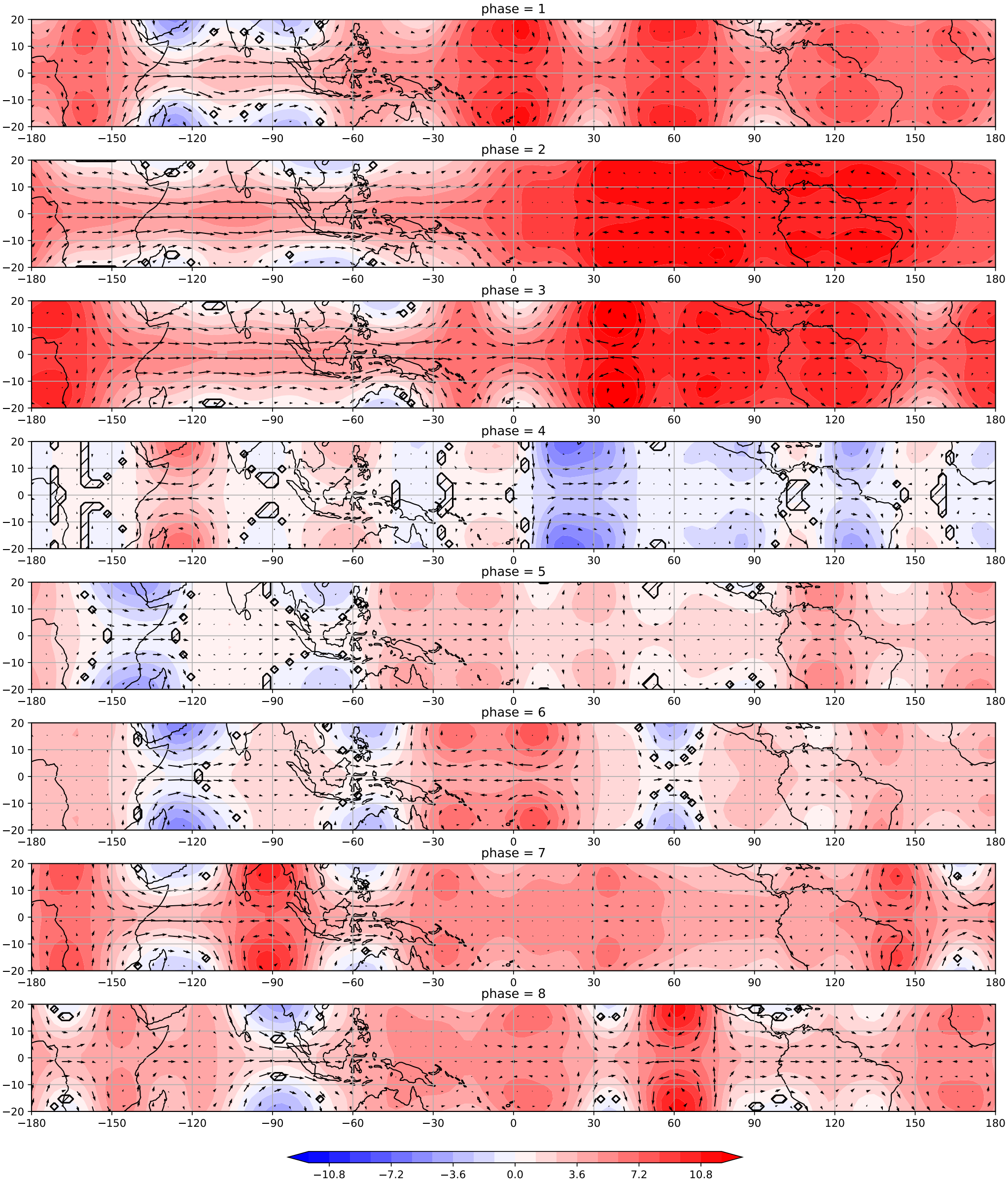

Figure 12. Figure 2.7.4: Difference between of the velocity and geopotential height fields associated with ROT modes with SZW30+ and SZW30-. The hatched region corresponds to significant difference of the geopotential height values under 5% confidence level.

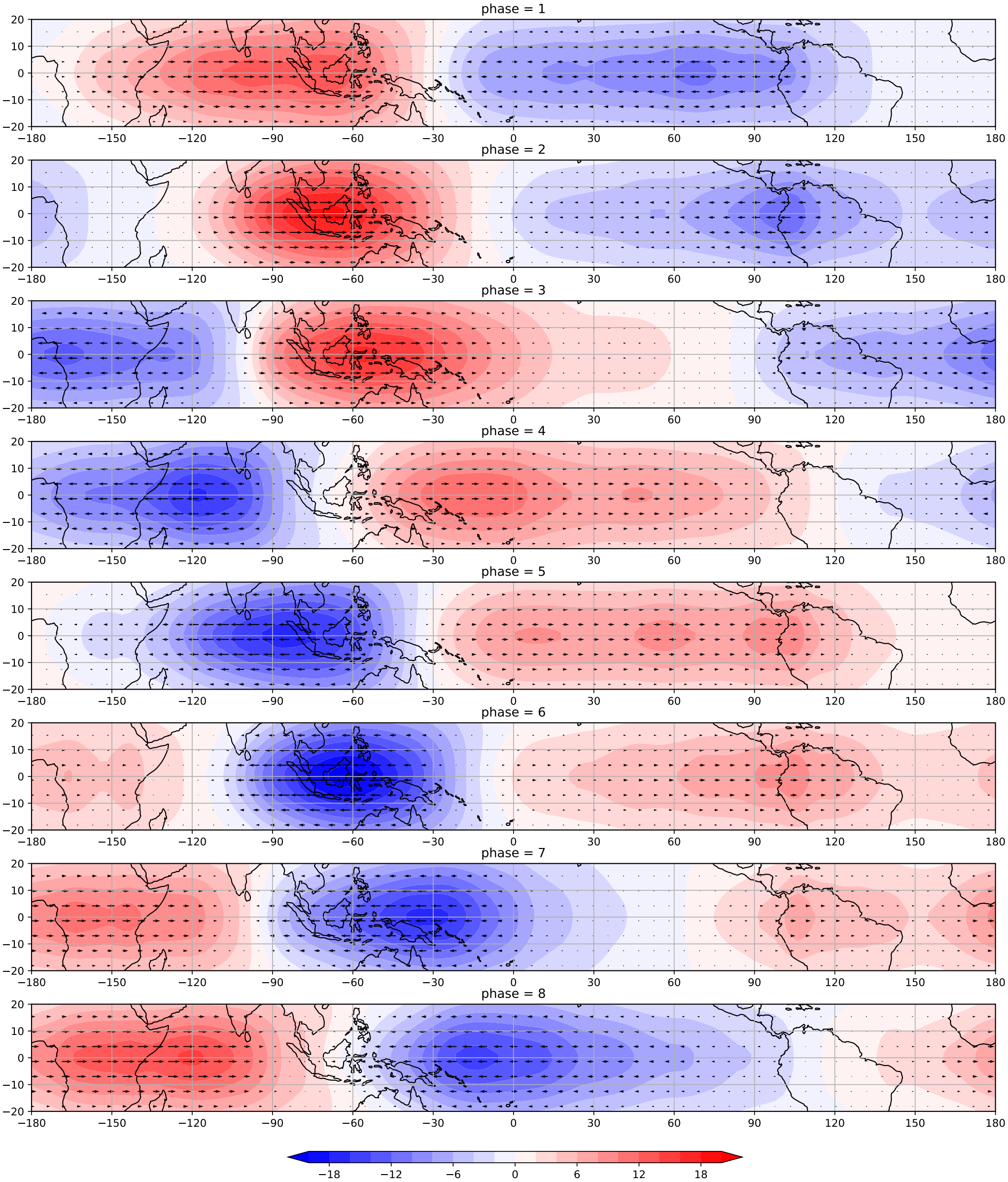

Figure 13. Reconstruction of the velocity and geopotential height fields associated with Kelvin modes with SZW30- at 200 Mb.

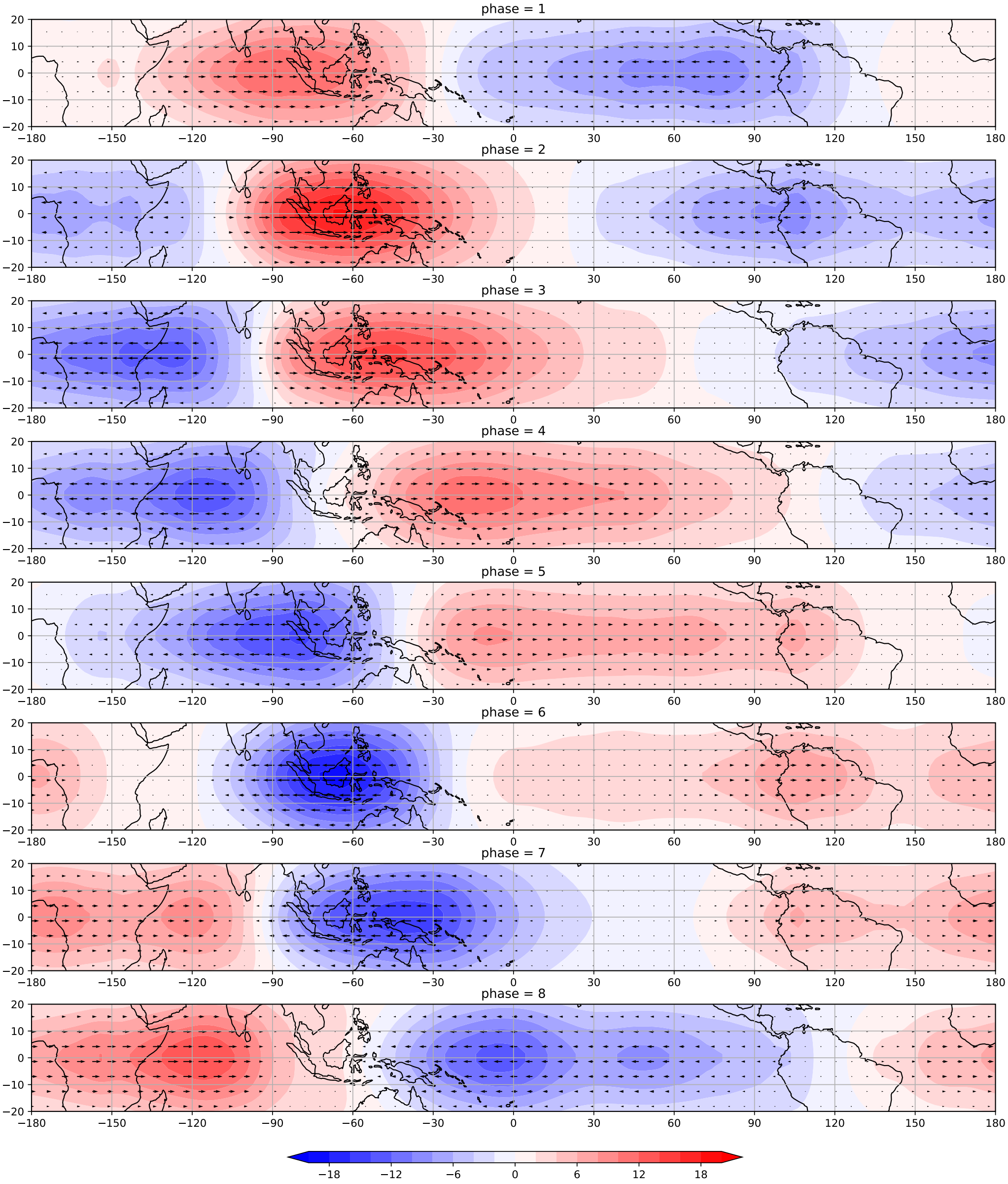

phase = 1

phase = 2

phase = 3

phase = 4

phase = 5

phase = 6

phase = 7

phase = 8

Figure 14. Reconstruction of the velocity and geopotential height fields associated with Kelvin modes with SZW30- at 200 Mb.

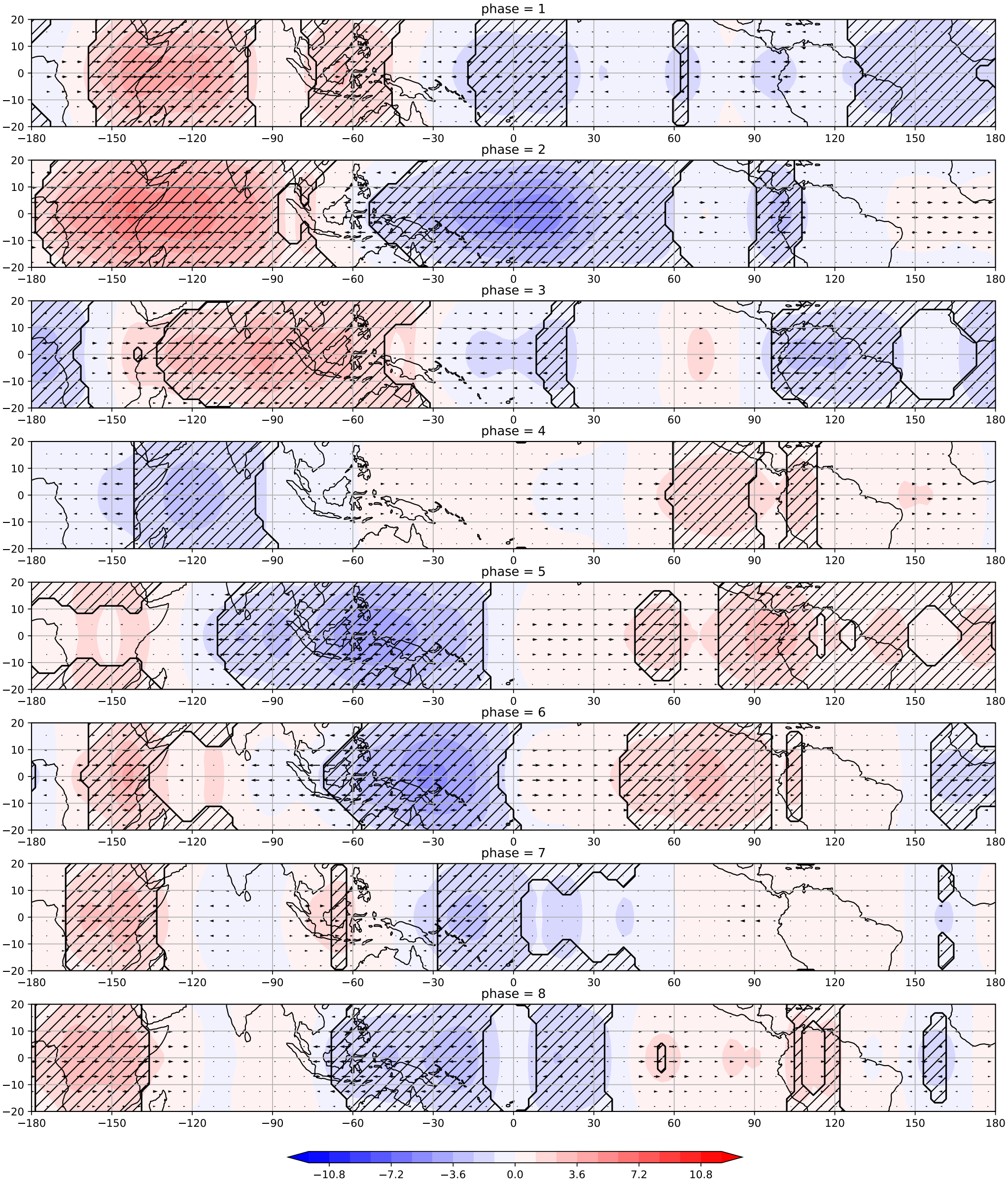

Figure 15. Difference between of the velocity and geopotential height fields associated with Kelvin modes with SZW30+ and SZW30-. The hatched region corresponds to significant difference of the geopotential height values under 5% confidence level.